

# **Sensitive Detection of Blood Biomarker Pentraxin 3 – Development and Comparison of Amperometric and Capacitive Biosensors in Flow-Injection Systems**



Author: Viktor Johansson

Performed at the Division of Biotechnology, Department of Chemistry

LTH Faculty of Engineering

at Lund University

September 2023

Supervisor: Associate professor Dr. Martin Hedström,

Examiner: Associate professor Dr. Javier Linares-Pastén

## **Acknowledgements**

This report is the final result of many months of hard work. It has been a tough learning experience, but I know for certain that it would be a lot harder without the people around me. I want to thank my family and friends for all the support. I would also give a special thanks my supervisor Martin for the countless hours of discussions and close cooperation in the project.

# Populärvetenskaplig sammanfattning

Mänskligheten strävar ständigt efter att utvecklas och bota olika typer av sjukdomar har varit ett prioriterat område i många hundra år. Idag har vi kommit långt, med många typer av olika antibiotika, målsökande terapier och vacciner. Men för att effektivt kunna behandla sjukdomar krävs att rätt diagnos ställs tidigt.

I detta examensarbete har jag utvecklat känsliga analysmetoder som kan ligga till grund för framtida klinisk diagnostik för tidig detektion av framför allt blodförgiftning (sepsis) men även andra sjukdomar som covid 19 och vissa typer av cancer.

För att kunna upptäcka en sjukdom eller infektion i kroppen krävs att man letar efter något som utmärker sjukdomen från allt annat, en så kallad biomarkör. I detta fall så har jag fokuserat på detektion av en biomarkör som heter pentraxin 3 eller PTX3. PTX3 produceras i kroppen som svar på vissa typer av infektioner och hjälper till att hitta den infekterande organismen och aktivera immunförsvaret i en tidig fas. Normalt sett finns PTX3 i låga nivåer i blodet, oftast under tre nanogram per milliliter, men nivåerna kan öka nästan 1000-faldigt vid en akut infektion. Att leta efter en så liten mängd är ungefärligt jämförbart med att leta efter en droppe i en simbassäng som är 50x25m.

För att hitta så små koncentrationer av PTX3 krävs ett väldigt känsligt analysystem som kan fånga in och mäta mängden. Till detta så används en elektrod med en guldyta som täckts av ett mycket tunt lager av antikroppar, kroppens bästa målsökarmolekyler. Antikroppar har en extremt bra förmåga att binda starkt och specifikt till målmolekyler (antigen), alltså i detta fall bara precis den biomarkören vi söker, PTX3, och hålla kvar den tills vi hunnit mäta hur mycket som finns i provet.

Att arbeta i en så liten skala gör att det krävs mycket känsliga mätmetoder och precisa injektionssystem. Jag använder i detta arbete ett flödesinjektions system (flow-injection analysis, förkortat: FIA) för att precis styra vilka volymer och flöden (mikroliter per sekund) som används. För att mäta mängden PTX3 så används två elektrokemiska mätmetoder som inte använts för denna biomarkör förut. Amperometrisk mätning som mäter hur mycket ström som kan passera ytan när man lägger på en bestämd spänning, och kapacitiv mätning som analyserar hur mycket ytan kan laddas upp, ungefär som ett pyttelitet batteri.

Resultaten i detta arbete tyder på att PTX3 binder till antikropparna på elektroden i kapacitiva systemet dessutom binder PTX3 hårt och är svårt att få loss så man inte kan mäta flera prov på samma elektrod. Dock så syns en inbindning även vid extremt låga koncentrationer vilket gör att man med ett optimerat system skulle kunna använda mycket små provvolymer och därmed späda bort mycket av det som stör analysen, d.v.s. annat som finns i t.ex. blodprov. Det amperometriska systemet är känsligt och verkar inte ha problem med stark inbindning och visar tecken på att det skulle kunna vara möjligt att mäta PTX3 i olika mängder.

Denna studie ska ses som ett första steg för dessa två metoder att kunna bli applicerbara i en klinisk miljö. Det finns mycket arbete kvar för att förbättra signaler och visa med hög säkerhet att det bara är PTX3 som binder, och att man kan göra kvantitativ (bedöma hur mycket) analys.

# Table of Contents

Acknowledgements .....	ii
Populärvetenskaplig sammanfattning .....	iii
Table of Contents .....	iv
Abbreviations .....	vi
Abstract .....	vii
1. Introduction .....	1
1.1 Clinical diagnostic .....	1
1.1.1 Sepsis .....	1
1.2 Biomarkers .....	1
1.2.1 Current analytical methods .....	2
1.2.2 Current research .....	2
2. Background and objectives .....	3
2.1 Pentraxin 3 .....	3
2.2 Bioanalytical chemistry .....	3
2.2.1 Flow-injection analysis (FIA) .....	4
2.2.2 Biorecognition element .....	5
2.2.3 Immobilization and functionalization of electrode .....	5
2.2.3.1. Electrode .....	5
2.2.3.2. Functionalization and immobilization .....	6
2.2.4 Detection principles .....	8
2.2.4.1. Cyclic voltammetry .....	8
2.2.4.2. Amperometry .....	9
2.2.4.3. Capacitance .....	10
2.2.4.4. ELISA .....	12
3. Materials and method .....	13
3.1 Chemicals and other material .....	14
3.2 Calculations .....	14
3.3 Methods .....	15
3.3.1 Instrumentation and setups .....	15
3.3.1.1. FIA-system .....	15
3.3.1.2. Electrode design and immobilization .....	18
3.3.1.3. Flow cell .....	20

3.3.2 Detection methods .....	21
3.3.2.1. Cyclic voltammetry .....	21
3.3.2.2. Amperometry .....	21
3.3.2.3. Capacitive biosensor analysis.....	23
3.3.2.4. ELISA type analysis.....	23
4. Results and discussion.....	24
4.1 Characterization of electrodes .....	24
4.2 Protein G model system .....	27
4.3 Capacitive measurements of PTX3 .....	29
4.4 Amperometry-preface .....	34
4.5 Amperometry PTX3 .....	36
4.6 Binding .....	38
4.7 Comparison of systems .....	39
4.8 Conclusion.....	39
5. Future perspectives.....	40
6. References .....	41
7. Appendix .....	43
7.1 Electrode overview .....	43
7.2 Protocols.....	46
7.2.1 Protocol self-assembling monolayer .....	46
7.2.2 Protocol electropolymerization .....	46
7.3 Figures .....	47
7.4 MATLAB scripts.....	48

## Abbreviations

<b>Ab</b>	Antibody
<b>CRP</b>	C-reactive protein
<b>DB</b>	Detection buffer
<b>DPV</b>	Differential pulse voltammetry
<b>EDC</b>	1-ethyl-3-(3-dimethylaminopropyl)carbodiimide hydrochloride
<b>EDL</b>	Electrical double layer
<b>EP</b>	Electropolymerized
<b>Fc</b>	Fragment crystallizable
<b>FIA</b>	Flow-injection analysis
<b>Fv</b>	Fragment variable
<b>HRP</b>	Horseradish peroxidase
<b>LOD</b>	Limit of detection
<b>MQ</b>	Milli Q
<b>NHS</b>	N-hydroxysuccinimide
<b>ON</b>	Overnight
<b>PG</b>	Protein G
<b>PRM</b>	Pattern recognition molecule
<b>PTX3</b>	Pentraxin 3
<b>RB</b>	Running buffer
<b>RT</b>	Room temperature
<b>SAM</b>	Self-assembled monolayer
<b>SIA</b>	Sequential injection analysis
<b>SPE</b>	Screen-printed electrode
<b>SPR</b>	Surface plasmon resonance
<b>TMB</b>	3,3',5,5'-Tetramethylbenzidine

## Abstract

Within clinical diagnostics there is always a need for innovative methods that are rapid, sensitive, and more accurate. In this study two bioanalytical systems have been evaluated for pentraxin 3 (PTX3) detection. PTX3 is a blood biomarker involved in the native immune system that can indicate sepsis, a disease that currently lacks a fast and sensitive analytical method for early detection. Currently, a whole panel of tests supported by physical symptoms is used, and diagnosis can only be confirmed several days after the blood sample is taken. PTX3 can also indicate other diseases such as covid 19 and some types of cancer. The analytical platforms in this work all utilize immobilized anti-PTX3 antibodies immobilized on an electropolymerized gold working electrode in combination with flow-injection analysis (FIA) to control the injections into a flow-cell with a three-electrode system. The first method used capacitance measurements and the results indicate that there is binding for PTX3 concentrations as low as  $10^{-20}$  M in buffer. The second system utilizes amperometric measurements and results point towards binding at concentrations of  $10^{-12}$  M of PTX3. Additionally, a capacitive model system with Protein G (PG) as an immobilized biorecognition element produced a clear signal when injecting  $10^{-13}$  M antibodies as a target.

# 1. Introduction

## 1.1 Clinical diagnostic

There has always been a strive for faster, more accurate and sensitive diagnostics to enable early treatment of patients and thereby save lives. Traditionally, as well as currently, methods used in clinical settings often rely on different chemical or microbiological assays, which typically are well performing in their respective areas. There is indeed a need for the detection of more complex molecules, such as specific biomarkers or pathogens. However, these methods often fall short on sensitivity, specificity, accuracy, or analysis time. Bioanalysis has the potential to fill this gap in the clinic (1, 2).

### *1.1.1 Sepsis*

One of the gaps in current clinical analysis is the diagnosis of sepsis, where currently the gold standard is to do a blood culture, a procedure that can take several days (3, 4). This timeframe is highly unfavourable since disease progression significantly increase the mortality. Instead, the diagnosis is based on several more general markers and symptoms (3). It is therefore of utmost importance that faster markers, or more accurate ones can be used to be able to issue the correct treatment in time, and increase the survival rate (5).

Sepsis is not a straightforward diagnose pointing towards a specific root cause, but rather can be seen as a broader term, describing the host response towards an infecting pathogen. The diagnosis can be split into sepsis and septic shock (6). The diagnostic problem lies in the very nature of the diagnose, it can be caused by many different types of pathogens.

## 1.2 Biomarkers

Each pathogen has a unique set of biomarkers that potentially could be used for identification, such as a specific set of DNA, RNA, or toxins. The most reliable biomarker for a pathogen is obviously the pathogen itself. Some pathogens can be identified by for example cultivating a sample. The other type of biomarker that can be used are the innate compounds that are produced in response or as a result of the infection. The theory being that each pathogen produces a certain response pattern that can be identified on a disease-by-disease basis.

The current biomarkers tested when suspecting sepsis are haemoglobin, leukocytes, thrombocytes, sodium, potassium, creatinine, thrombin coagulation times, CRP, bilirubin, glucose, blood gases and lactate. These are not definitive and only a combined picture with symptoms and physical parameters are enough to diagnose sepsis with decent accuracy (3). There are however emerging potential biomarkers that can improve accuracy and differentiate between the types of sepsis, this especially if the markers are combined and used in a scoring system (7).

One of the markers that has the potential to improve sepsis diagnostics is PTX3 (8).



### *1.2.1 Current analytical methods*

The current analytical methods that use existing biomarkers are typically standardized (often with a high level of automation) and large manufacturers of diagnostic equipment such as Siemens and Abbot have well documented and verified assays that are used, and many of the laboratories using these systems are accredited.

There are different ways to solve the sepsis diagnosis problem whereof the most notable is to use PCR and magnetic particles with a magnetic resonance detector to be able to identify which species of bacteria or fungi that has infected the patient. One such system has been approved by the FDA (9). This type of system is however limited to a finite number of predetermined pathogens. Other groups have focused on biomarkers of the host response since these has the potential to cover more infections, especially if combined. PTX3 has been included in several of these studies (10, 11).

### *1.2.2 Current research*

The most common method used for detection PTX3 is ELISA. This is a good method for measuring PTX3 levels and has been used extensively for research purposes. ELISA however has some drawbacks making it less suitable for future clinical applications (12).

Some alternative bioanalytical methods for detecting PTX3 has been proposed. For example surface plasmon resonance (SPR) (13) and differential pulse voltammetry (DPV) with gold nanowires (12). These have not reached the clinic. Other methods have not been reported on, notably amperometry and capacitance measurements. These methods have been successfully applied to other proteins and compounds and could potentially work for PTX3 (14, 15, 16).

The aim of this master thesis is hence to explore and propose the characteristics of a viable biosensor design for PTX3 detection, that could be suitable for use in clinical applications.

## 2. Background and objectives

### 2.1 Pentraxin 3

PTX3 is an acute-phase protein that is a part of the innate immune system that bridges the response to the adaptive immune system (17). The biomarker is normally present in very low concentrations (<3 ng/ml in plasma) (18) but increases up to 100-1000 ng/ml with some diseases. PTX3 is produced rapidly in response to infections, the levels starts to increase already within 6-8 h (17).

PTX3 levels has been linked to sepsis severity, and correlated with the severity in a number of other diseases such as cardiovascular disease and cancer, but also infections such as dengue virus and tuberculosis (17).

Research suggest that PTX3 is a octameric protein complex (19) with a structure seen in Figure 1 where each subunit is 381 amino acids long and has two distinct domains, the pentraxin-like domain and a long domain. These domains have several epitopes, for example a C1q binding domain and a pattern recognition domain. This makes the PTX3 molecule a pattern recognition molecule (PRM) that binds parts of some pathogens and also binds a complement system component, C1q and consequently activating the molecule (17). These characteristics makes PTX3 a good match for a bioanalytical approach and a valuable addition to existing biomarkers for several diseases.

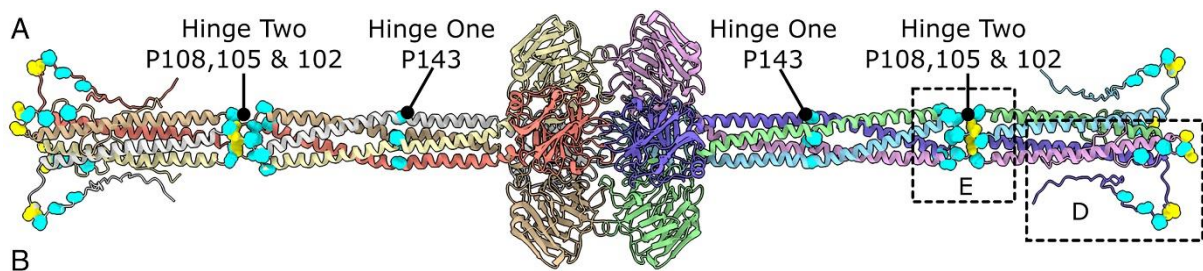


Figure 1: Octameric form of PTX3 (19).

### 2.2 Bioanalytical chemistry

Bioanalysis can be defined in two ways. The first interpretation of the definition is that the analyte has to be a part of or derived from a biological system. This includes detecting for example biomarkers or drugs with for example mass spectrometry. The second way of defining a bioanalysis is to interpret that the sensor element is derived from a biological system. This would include systems based on enzymes and antibodies, such as ELISA (20).

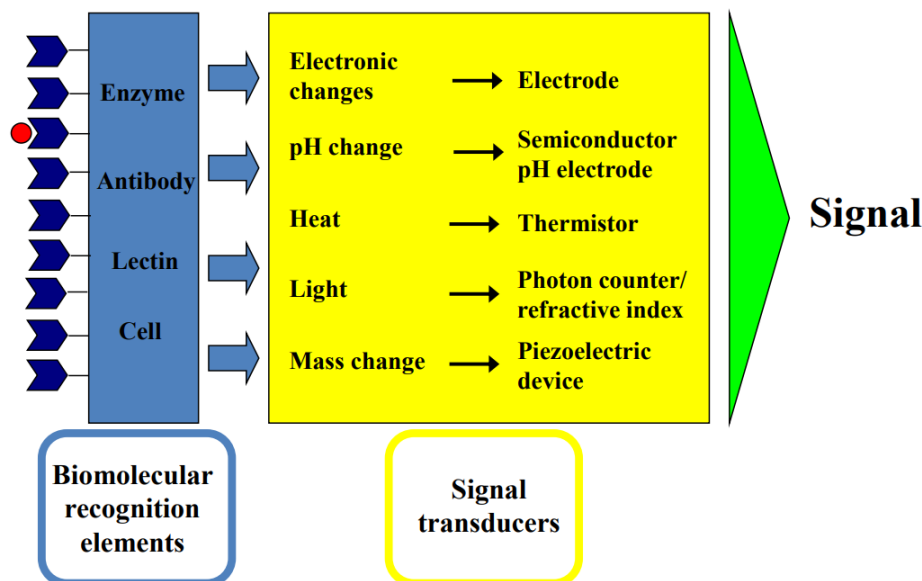


Figure 2: Overview of a biosensor (21).

For the second definition a biosensor contains two main parts seen in Figure 2, the biomolecular recognition element (biorecognition element) and the signal transducer. The biorecognition element needs to be able to capture the analyte to function, and the signal transducer needs to be able to react to a binding of analyte on the biorecognition element. Further, to create a readable response; the analyte, signal, and the electronics to interpret the signal also needs to be present.

### 2.2.1 Flow-injection analysis (FIA)

Flow injection analysis is an analysis methodology where the analyte is introduced into a continuous stream of carrier liquid that transports the sample to a flow cell where a detector is mounted. The sample is introduced into the closed system in a repeatable manner, which makes it possible to design a robust and sensitive system. The system is dependent on the low tolerances of its components to minimize errors, thereby reducing variability in measurements.

Important parameters that can be controlled in FIA is dispersion, residence time, mixing and total analysis time. These are highly dependent on the design choices in the development of the system and the demands of the sensor. Generally, low dispersion and short analysis time is ideal, however high flow gives shorter analysis time but increases flow. This highlights the need to optimize each parameter to the unique implementation (22).

There are similar techniques developed from FIA, such as sequential injection analysis (SIA) which builds on the principles but further miniaturizes the system and stores sample and buffer in an injection loop which is injected to the sensor. This approach minimizes the sample volume further than the FIA approach and improves other important aspects such as dispersion and dead volume (23).

### *2.2.2 Biorecognition element*

The most important feature of an analysis system is its ability to differentiate the analyte from the similar molecules and the sample matrix. For a biosensor, a biorecognition element is used for this purpose. This is often an antibody (Ab) or protein that has some specific binding properties towards the analyte.

Protein G and A are proteins that specifically binds the Fc part of antibodies with high affinity. Since they are readily available and can bind many commercial antibodies, they can be cost effective fast and early development of systems.

Antibodies is a part of the adaptive immune system and has the ability to be developed to bind almost any type of molecule. It is therefore very common and relatively simple to develop antibodies that bind a specifically to a desired molecule. The most common way is to expose an animal to the desired molecule, the antigen, then let the immune system react and lastly extract and purify the antibodies produced. This gives a mixture of antibodies that binds different parts of the antigen and also a mixture of antibody types. This means that the antibodies bind different parts of the antigen and that there is more variance when producing and using the antibodies (24).

The alternative is to produce monoclonal antibodies, using only a single antibody producing cell from an animal that has been exposed to the antigen and then creating a hybridoma by fusing it to a cell that can reproduce indefinitely.

For clinical purposes a monoclonal is preferred since the batch variation is vastly lower and quality over time is consistent since monoclonal antibodies interact with the same part of the analyte. A result that cannot be ensured when immobilizing polyclonal antibodies.

### *2.2.3 Immobilization and functionalization of electrode*

#### 2.2.3.1. Electrode

There are a lot of alternatives when choosing electrode types in analytical systems. There are differences in size, surface material and how the material is deposited on the surface. The size is determined by the type of system that it integrates with, while the material can be chosen for its electrical or chemical properties to fit the biorecognition element and sensor type.

Gold is a common material to use for the electrode surface. it has very good compatibility with a wide variety of surface chemistries and biorecognition elements and potential ranges. Gold is therefore likely to work in many different applications (16).

The most common type of electrode is the screen-printed electrode (SPE). For these electrodes the electrode material is deposited onto a ceramic or polymeric substrate as a form of ink with a mask covering the part where the ink should not be deposited (25). An alternative type is to use thermal evaporation and deposit gold on silica or glass (16).

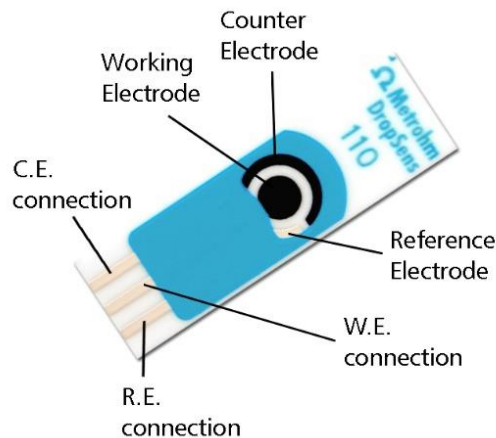


Figure 3: Typical screen printed electrode (26).

The screen-printed electrode seen in Figure 3 has an integrated three-electrode system and is cheap and commercially available with a wide variety of sizes and materials. The thermally evaporated electrode is harder to manufacture but has outstanding stability and reusability when combined with external reference and auxiliary electrodes.

### 2.2.3.2. Functionalization and immobilization

Most biorecognition elements cannot be optimally attached to a gold or carbon surface directly since it would be done by adsorption, leading to a random orientation of the biorecognition element. To circumvent this, some type of molecular handle is needed. Many options are available (shown in Figure 4), and some have advantages for different types of biorecognition elements. The core part of functionalization is that a chemical group that can further react and create a bond to bind the biorecognition molecule is introduced (27). This step will also affect the surface conditions since the functionalization will cover the original electrode surface and features such as resistance over the interface will be changed (16).

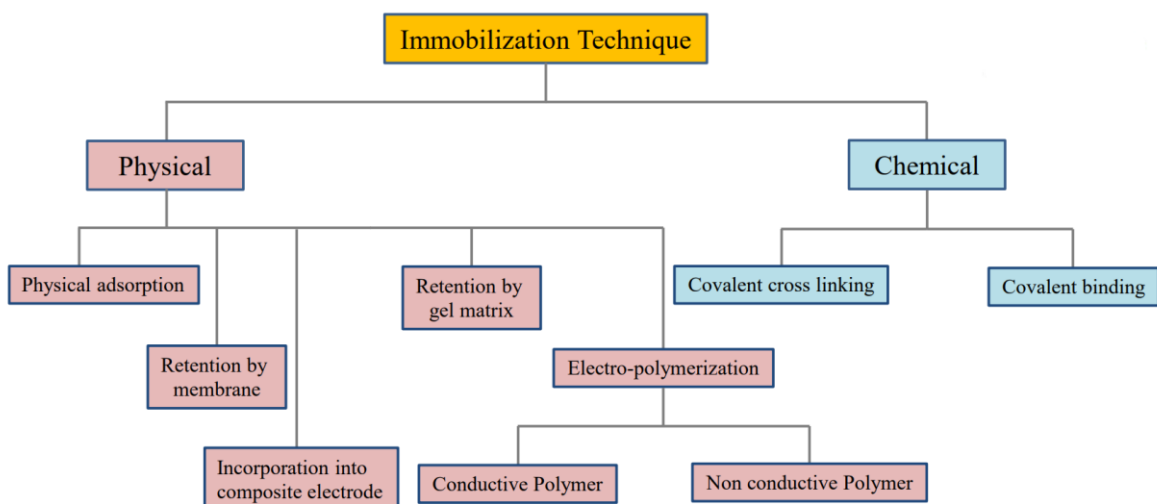


Figure 4: Overview of immobilization techniques (21).

Electropolymerization is an alternative to create a layer where biorecognition elements can be attached. To create the polymer, monomers with groups that can be electrically activated are dissolved in a solution and attached by varying the potential on the surface. This leads to oxidation of the monomers at the surface and then binding between the monomers. An example of a molecule that can be used in this way is tyramine (16, 20).

The thickness of the polymer can be altered by varying the number of potential sweeps, altering its characteristics. Commonly a thinner polymer produces a more sensitive surface with fast response while a thicker produces a sensor with higher response in absolute terms.

Self-assembling monolayers (SAM) is a phenomenon where molecules adsorb and organizes on for example a gold surface in a predictable manner. There are some types of molecules that can assemble in this way spontaneously, for example thiols, sulphides and disulphides whereof  $\alpha$ -lipoic acid is an example of the latter (16).

Connecting the biorecognition element to the surface or interface requires an immobilization technique. There are several choices for immobilizing antibodies and similar proteins some of the most common are covalent, oriented and non-covalent (27).

For biosensors with a design requirement for stability a covalent design is often preferred since the covalent binding is very strong comparably with some of the other techniques. The most common way of introducing a covalent bond between the functionalized surface and the biorecognition element is to use 1-Ethyl-3-(3-dimethylaminopropyl)carbodiimide (EDC) and N-hydroxysuccinimide (NHS) (27).

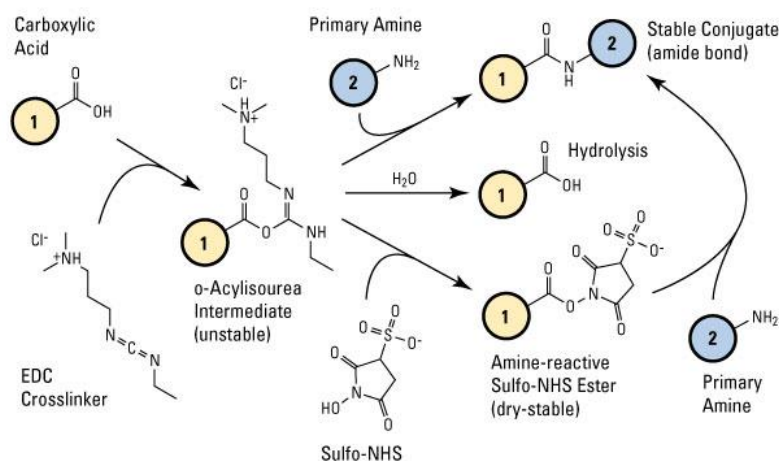


Figure 5: Mechanism of EDC NHS chemistry, in this illustration with sulfo-NHS (28).

The requirement is that there is a free carboxylic acid and free primary amine as seen in Figure 5 on the respective sites that are to be coupled. Mechanistically, EDC reacts with a free carboxylic acid on the protein or the activated surface and creates an unstable intermediate, this reacts with NHS and creates a semi stable molecule with a good leaving group that the amine can react with and create a strong amide coupling. Proteins often has both free primary amines and carboxylic groups while these can be introduced on the surface with a correct activation choice (29).

An oriented (site-directed) approach ensures that the active part of the biorecognition element is accessible for the analyte. It does however require an extra step where a molecule that can hold the biorecognition element is attached. The most common way to do this is to attach protein G or protein A. These proteins can bind the fragment crystallizable (Fc) part of antibodies on based on affinity, enabling the fragment variable (Fv) part of antibodies to bind the analyte. This technique however requires that the orientation molecule has been attached in beforehand by another technique (27).

A non-covalent approach is the easiest technique to introduce antibodies to a surface. It has very few restrictions regarding the biorecognition element or surface and involves only a couple of steps. However, it is also not very effective and the biorecognition element will be randomly oriented, increasing the likelihood of having the active part of the Ab inaccessible to the analyte (27).

### *2.2.4 Detection principles*

There are many ways of measuring the amounts of analytes in a matrix. However, there are a limited number that are both very sensitive and currently has the potential to be scaled in a way that is economically viable. Spectrophotometric methods for example often have a limited sensitivity or limit of detection (LOD) while the most advanced methods such as mass spectrometry has cost and sample purity limitation. Electrochemical techniques are an alternative that theoretically combines the simplicity of the spectrophotometric methods with an excellent sensitivity (12, 30).

#### *2.2.4.1. Cyclic voltammetry*

Cyclic voltammetry is a technique that in its basic form sweeps a range of potentials over a working electrode and measures the responding current. This is done cyclically, meaning each potential will be measured twice, apart from the lower and the upper endpoints. This technique is commonly applied to investigate surface, and redox reaction characteristics (31).

To be applicable, an electroactive compound that can react to the potential needs to be present in the solution. The compound is reduced and oxidized as a result of the applied potential and the condition of the surface. A more isolated surface results in less reduction and oxidation and this in turn gives a lower current (14, 31).

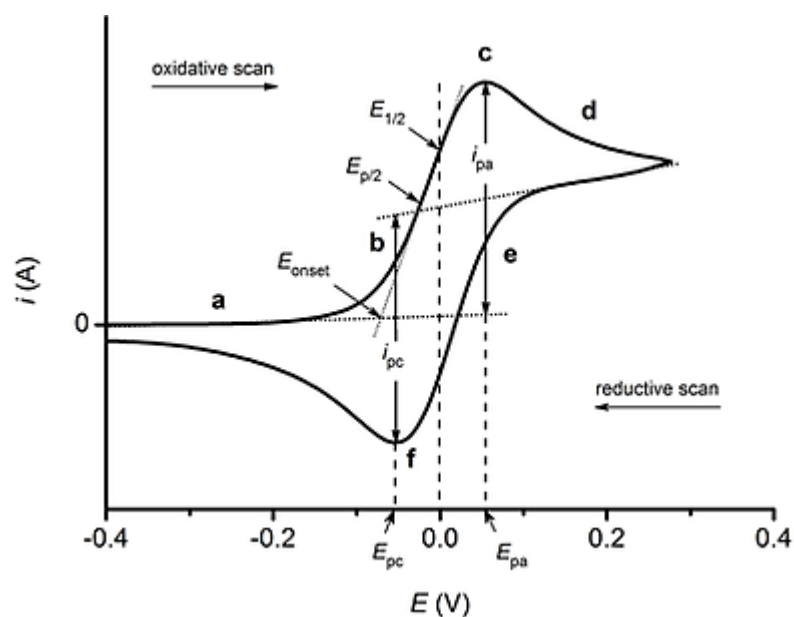


Figure 6: Typical cyclic voltammetry diagram with oxidation  $i_{pa}$  (top) and reduction  $i_{pc}$  (bottom) peaks.(32).

A compound that can be used is potassium hexacyanoferrate  $K_3[Fe(CN)_6]$ . This compound has two oxidation states for the  $Fe(CN)_6$ . The first is -3 and when reduced it has a charge of -4. If no potential is applied the two states will be in equilibrium, but if a potential is increased or reduced the equilibrium will shift. In the graph for a cyclic voltammetry this is seen as an increasing or decreasing current (Figure 6).

#### 2.2.4.2. Amperometry

Amperometry is an electrochemical measurement method which measures the current (in amperage) going through a working electrode when applying a potential. This can be used for either measuring electrically active reactions or species. The compounds are oxidized or reduced by increasing or reducing the potential and generates a faradic current that is proportional to the amount present.

At a constant potential and experimental environment, the electron transfer will be determined by mass transfer. That in turn depends on the area and concentration of analyte. Amperometry can effectively distinguish between electroactive species by choosing the appropriate applied potential depending on the oxidation and reduction potential of the analyte and interfering species. Additionally, electrode material and additives to the solution can increase the potential to differentiate between species.

The compatibility and optimum potential for the system can be effectively tested by obtaining a voltammogram (33).



### 2.2.4.3. Capacitance

Capacitance is a measurement of how much electrical energy (i.e. charge) a component can hold and is measured in Farads. In the conventional electronic components, a capacitor is charged by applying a potential, current will flow into one side of the capacitor. However, since the two sides of a capacitor is separated by a dielectric material that does not conduct current, charges will be separated and thereby energy will be stored.

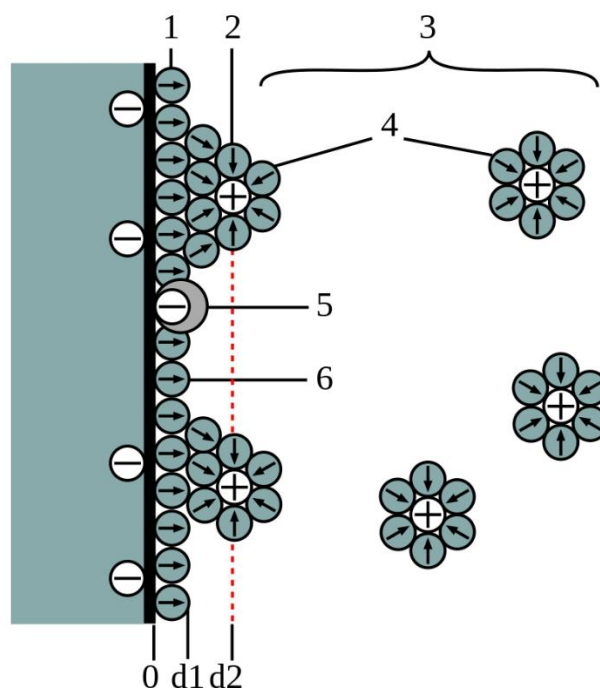


Figure 7: Schematic representation of a double layer on an electrode (BMD) model. 1. Inner Helmholtz plane, (IHP), 2. Outer Helmholtz plane (OHP), 3. Diffuse layer, 4. Solvated ions (cations) 5. Specifically adsorbed ions (redox ion, which contributes to the pseudocapacitance), 6. Molecules of the electrolyte solvent (34).

For a biosensor the analogue to the capacitor is the electrical double layer. The electrical double layer (EDL) was described first by Helmholtz 1879 and was further improved by Gouy and Chapman, and later Grahame. This model describes two layers on the interface between an electrode and a liquid with electrolytes. The inner layer that is called the Stern layer (or Helmholtz layer) and an outer layer called Gouy- Chapman diffuse layer as seen in Figure 7.

The Stern layer is split into two parts: the inner Helmholtz plane and the outer Helmholtz plane. The inner Helmholtz plane contains specifically adsorbed ions and solvent species and is only one molecule thick. The outer Helmholtz plane consists of ions that has been solvated and that interact electrostatically with the molecules of the inner Helmholtz plane. The outermost layer against the bulk solution, the Gouy Chapman diffuse layer contains mobile ions that are affected by both electrostatic and diffusion (16, 35).

These layers act as capacitors in series if no charge is transported across the interface holding charge when a potential is applied. A well isolated layer between the electrode and the Helmholtz layer can create these conditions.

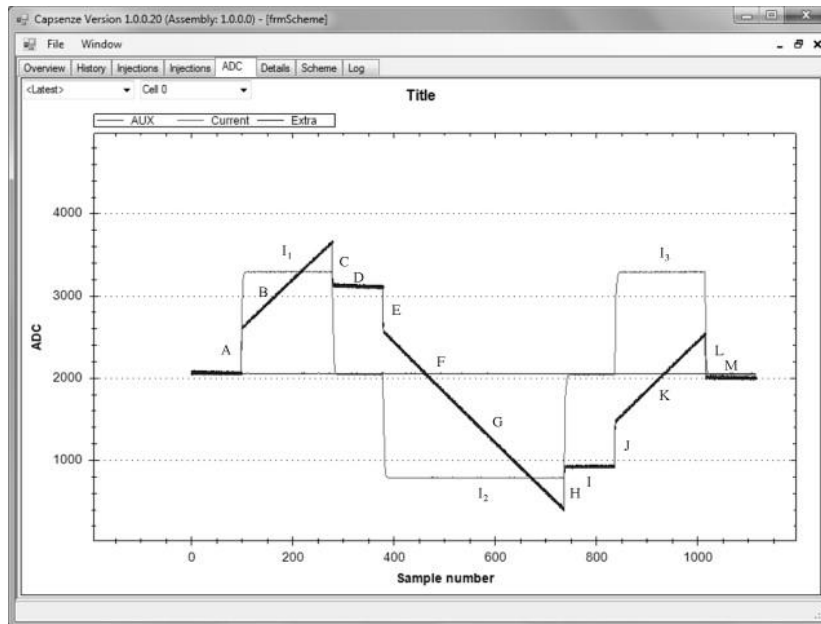


Figure 8: Overview of an ideal single measurement of capacitance on electrode (36).

The capacitance can also be measured by pulsing a constant current and this has been shown to increase the stability of the signal. The capacitance is calculated from three sub pulses shown in Figure 8 as  $I_1$ ,  $I_2$  and  $I_3$  and the respective potential response labelled A-M (36).

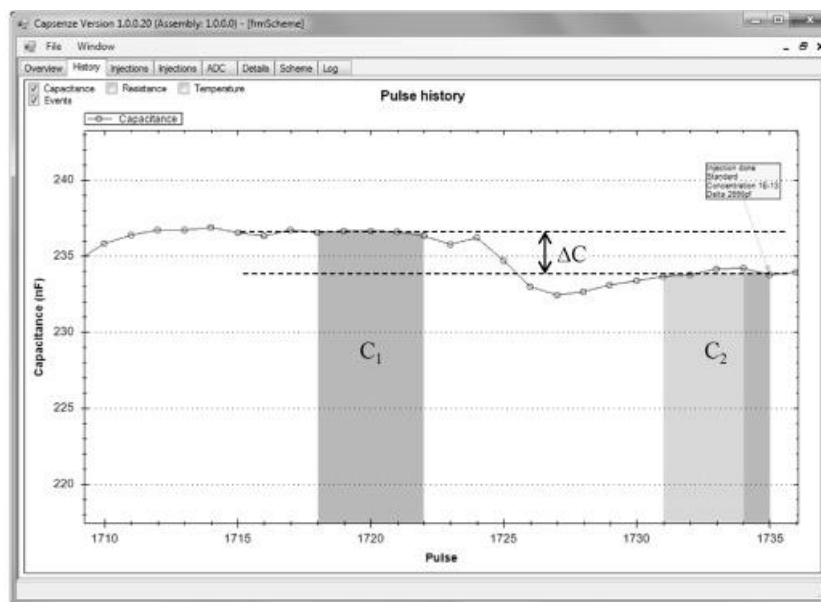


Figure 9: Visualization of capacitance signal calculation for binding on electrode (36).

To measure the capacitance signal from binding on an electrode the difference between capacitance before and after the injection is calculated. This is done by using two averages for the baseline before and after injection (Figure 9).

### 2.2.4.4. ELISA

Horse radish peroxidase (HRP) and its electroactive substrate 3,3',5,5'-tetramethylbenzidine (TMB) together with H<sub>2</sub>O<sub>2</sub> is a common combination to measure amount of bound analyte in ELISA and it is commonly measured spectrophotometrically. HRP oxidizes TMB from colourless to its first oxidized state which is blue/green as seen in Figure 10. The reaction is then stopped by adding acid which pushes the TMB to its most oxidized state which is yellow seen in Figure 11.

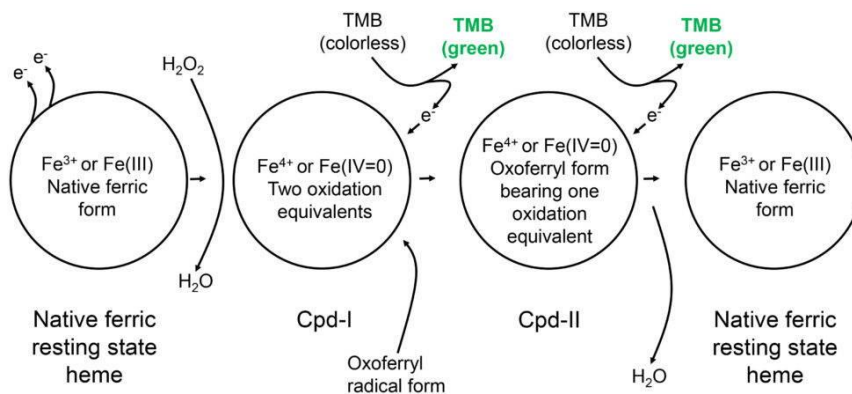


Figure 10: Interaction between HRP, H<sub>2</sub>O<sub>2</sub> and TMB (37).

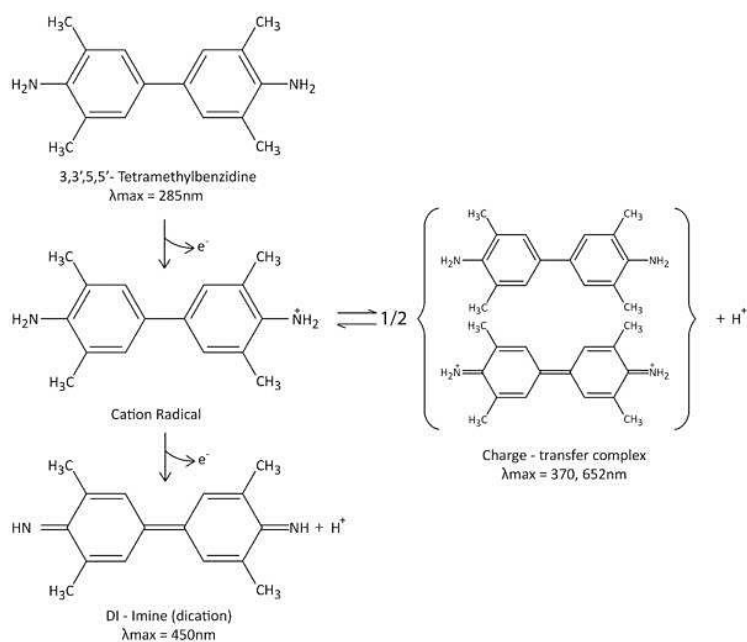


Figure 11: Oxidation states of TMB (37).

### 3. Materials and method

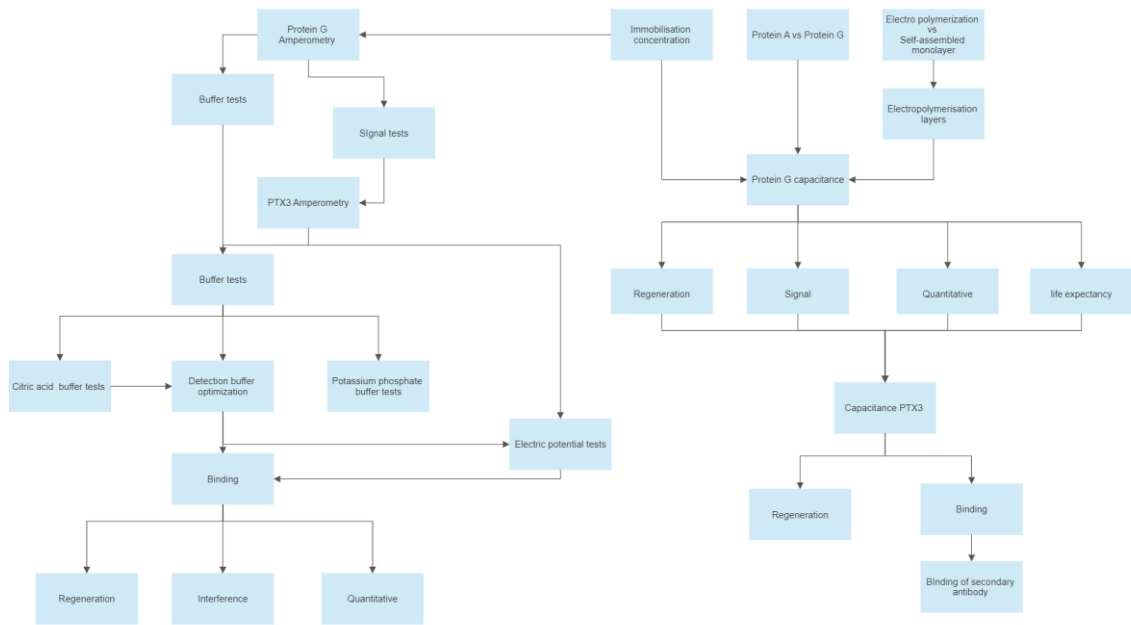


Figure 12: Overview of experiments performed. Only some results are discussed in this report.

### 3.1 Chemicals and other material

Table 1: Chemicals used.

Chemical	Supplier
EDC (1-ethyl-3-(3-dimethylaminopropyl) carbodiimide hydrochloride)	Fisher scientific
NHS (N-hydroxysuccinimide)	Fisher scientific
(+)- $\alpha$ -Lipoic acid	Sigma Aldrich
1-Dodecanethiol	Sigma Aldrich
Tyramine, 98+%	Thermo Scientific Chemicals
Ethanolamine ACS reagent, $\geq 99.0\%$	Sigma Aldrich
Methanol ACS reagent, $\geq 99.8\%$	Sigma Aldrich
Potassium hexacyanoferrate(III) ACS reagent, $\geq 99.0\%$	Sigma Aldrich
Potassium phosphate dibasic	Sigma Aldrich
Potassium phosphate monobasic	Sigma Aldrich
Anti-Pentraxin 3 antibody, Rabbit Polyclonal (12082-RP02)	Sino Biological
HRP-conjugated rabbit polyclonal antibody to human Pentraxin 3 (PTX3) (LS-C670898) (0.33 mg/ml)	LifeSpan Biosciences
Pentraxin 3 Protein, Human, Recombinant (His Tag) (12082-H08H) (50 $\mu$ g resuspended in 200 $\mu$ l MQ)	Sino Biological
Protein G	GenScript
Polyclonal goat anti-mouse immunoglobulins	DakoCytomation
H <sub>2</sub> O <sub>2</sub> , 30% (W/W)	Sigma
Polyclonal swine anti-rabbit immunoglobulins HRP (1.4 g/l)	Dako
Rabbit Polyclonal immunoglobulins	Kind gift from Genovis AB
3,3',5,5'-Tetramethylbenzidine (TMB) liquid substrate, supersensitive for ELISA	Sigma life science

All other chemicals were of analytical grade.

The water was Milli Q processed with 0.22 $\mu$ m filter.

### 3.2 Calculations

Calculations of concentrations for the antibodies and proteins are calculated from the stock concentration in grams per ml that has been available on the original container or the recommended resuspension in the documentation. Dilutions are noted as the number that has to be multiplied with the stock concentration to have the new concentration.

## 3.3 Methods

### 3.3.1 Instrumentation and setups

Instrumentation, lab facilities and chemicals were kindly provided by the division of biotechnology at Lund University and Capsenze AB.

#### 3.3.1.1. FIA-system

Four types of injection systems were used when evaluating the biosensor and the measurement methods. The simplest system used only a syringe to inject sample into a flow cell connected to AUTOLAB PGSTAT302N (Figure 13). For this system the NOVA 2.1.6 software from Metrohm that controls the Autolab was used for analysis setup and data extraction.

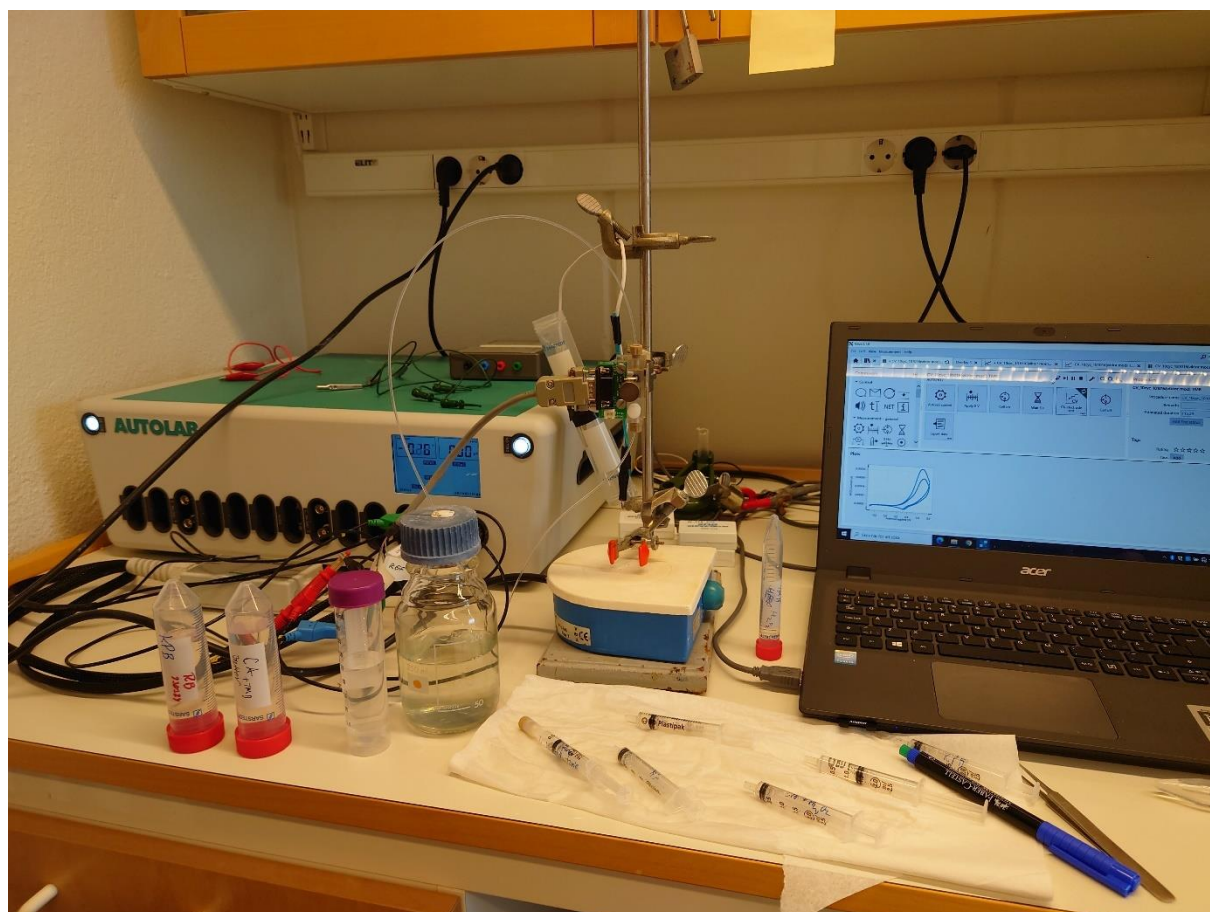


Figure 13: Manual injection setup connected to Autolab PGSTAT 302N.

The second system seen in Figure 14 used a Lambda miniplus3 peristaltic pump and a manually controlled pneumatic injection valve, this was connected to an external AUTOLAB PGSTAT302N for amperometric measurement. For this system the NOVA 2.1.6 software from Metrohm that controls the Autolab was used for analysis setup and data extraction.

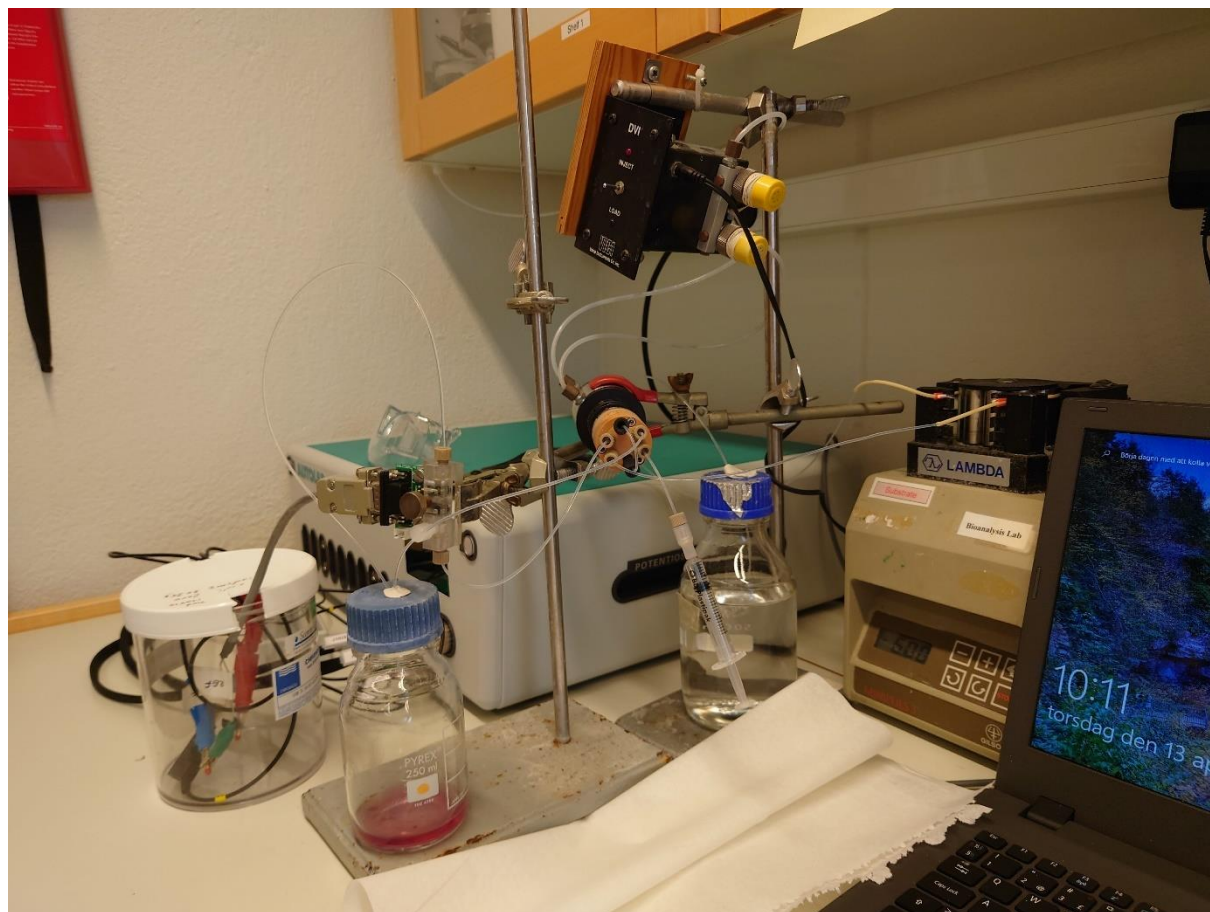


Figure 14: Pneumatic valve setup with peristaltic pump and connected Autolab PGSTAT 302N.

The next system seen in Figure 15 was a small integrated FIA system from Capsenze with a 12-port valve and a Tecan syringe pump and a degasser. A flow cell was connected to the machines biosensor port that could calculate the signal with the accompanying Capsenze software. The Capsenze software was used to create running schemes and collect data, however the raw data was further processed and displayed by using a MATLAB script (see Appendix).



*Figure 15: Smaller Capsenze system with integrated biosensor.*

The most advanced and flexible system was a FIA system from Capsenze (Figure 16) which incorporates, dual Tecan syringe pumps, dual 12-port valves, a degasser, possibility for biosensor mounting, a spectrophotometric module, a Peltier element, and three 3-way valves. The Capsenze web interface was used to create running schemes and collect data.



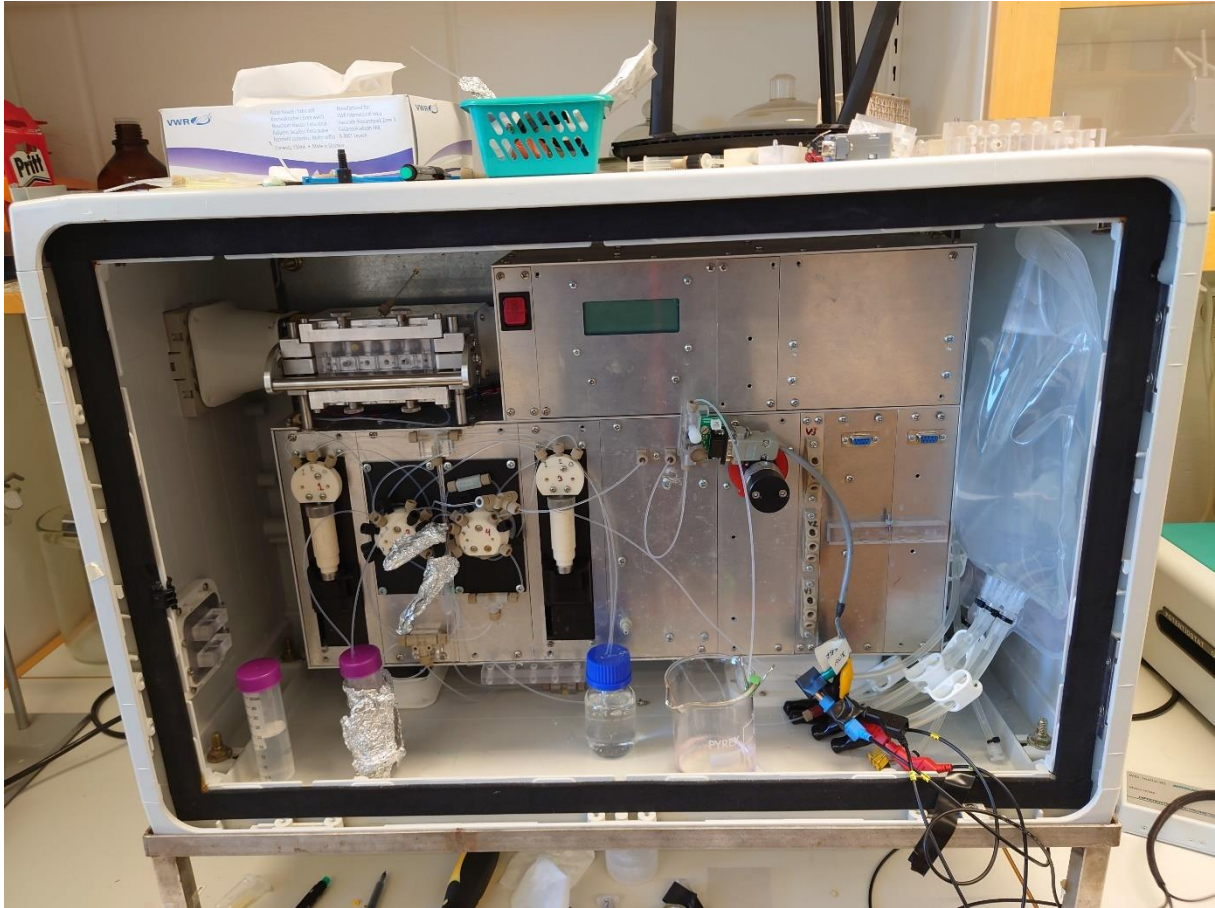


Figure 16: Advanced Capsenze FIA-system.

### 3.3.1.2. Electrode design and immobilization

All electrodes used had been manufactured earlier in-house using thermal evaporation of gold on silica wafers. The electrodes have a 3 mm in diameter circular gold surface for immobilization.

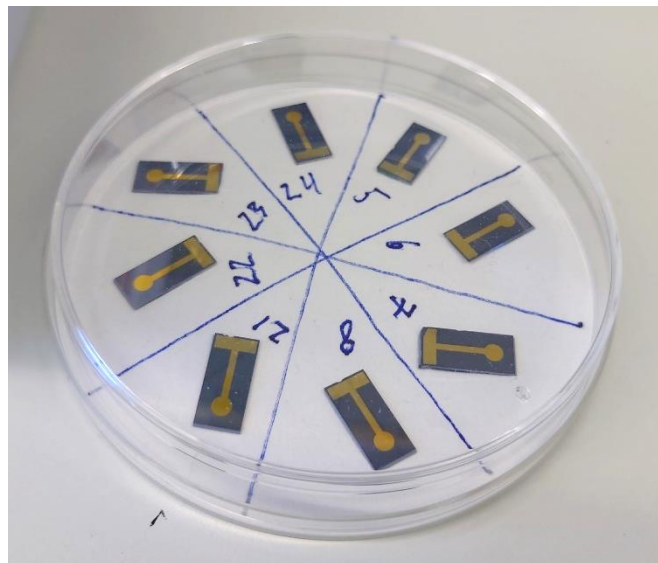


Figure 17: Electrodes protected from contamination in petri dish.

Electrodes were first separated from their wafer by breaking it along pre-etched lines and thereafter placed in a petri dish with a lid for protection against e.g. dust particles (Figure 17). The next step was to thoroughly clean the gold transducers by adding 25  $\mu$ l piranha solution 3:1 ( $H_2SO_4$  to  $H_2O_2$ ) for 10min. The electrodes were then washed with Milli Q (MQ) treated water and dried with  $N_2$  gas before being put in Eppendorf tubes filled with  $N_2$  gas. Each electrode received an ID depending on surface treatment and batch e.g., EP2B would be electropolymerized electrode 2 in batch B.

For the surface functionalization, two different methods were used. The first is functionalization by using SAM. The cleaned electrodes were thoroughly flushed with ethanol and immediately put in Eppendorf tubes with  $\alpha$ -lipoic acid 2% w/w in ethanol for 24h. The electrodes were then washed again with ethanol and dried with  $N_2$  before the immobilization step.

The second surface functionalization method is electropolymerization and was performed by filling a small beaker with 0.1 M tyramine and 0.3 M NaOH in methanol. The beaker was placed under a 3-electrode setup; Ag/AgCl reference electrode, a platinum auxiliary electrode and crocodile clamp that was connected to the working electrode that is to be polymerized (Figure 18).



Figure 18: Experimental setup for cyclic voltammetry. In front: crocodile clamp with attached working electrode, right Ag/AgCl reference electrode, in the back is the Pt auxiliary electrode.

The electrode setup was connected to the AUTOLAB PGSTAT302N with a computer and NOVA 2.1 software. A custom cyclic voltammetry that starts on 0 V and cycles up to 1.5 V and down to 0.05 V with 50 mV/s before returning to the start. This was repeated for the desired number of cycles. The electrodes were then washed again with ethanol and dried with N<sub>2</sub> before the immobilization step.

Frozen aliquots of EDC and NHS was thawed and readily suspended in MQ water to reach concentrations of 0.4 M and 0.1 M. EDC and NHS was then mixed 1:1 before 25 µl were pipetted onto the electrode and incubated 1 h in room temperature (RT).

The electrodes were then washed with MQ and Potassium phosphate buffer pH 7.4 10 mM and dried before 25 µl of fresh biorecognition element in Potassium phosphate buffer pH 7.4 were pipetted onto the electrodes and incubated dark overnight (ON) or weekend in fridge.

Lastly the electrodes were washed with MQ and Potassium phosphate buffer pH 7.4 10 mM with 0.005% V/V tween also referred to as running buffer (RB) before being put in tubes with RB for storage in the fridge.

Most electrodes used for capacitance measurement were dried, washed with ethanol and then treated with 10 mM 1-dodecanethiol in ethanol for 10min RT before being washed again with ethanol, dried and then washed with MQ and RB before being used.

### 3.3.1.3. Flow cell

The flow cell used (Figure 19) has been designed to hold two working electrodes and has a three-electrode design, where reference and the auxiliary electrodes were made of platinum. The two cells are positioned in series and the whole flow cell is reversible, meaning the inlet flow can be mounted on either side, depending on which electrode that the flow should meet first. The flow cell can be used either in single or dual working electrode configuration, although an inactive electrode always has to be mounted to seal the flow cell.

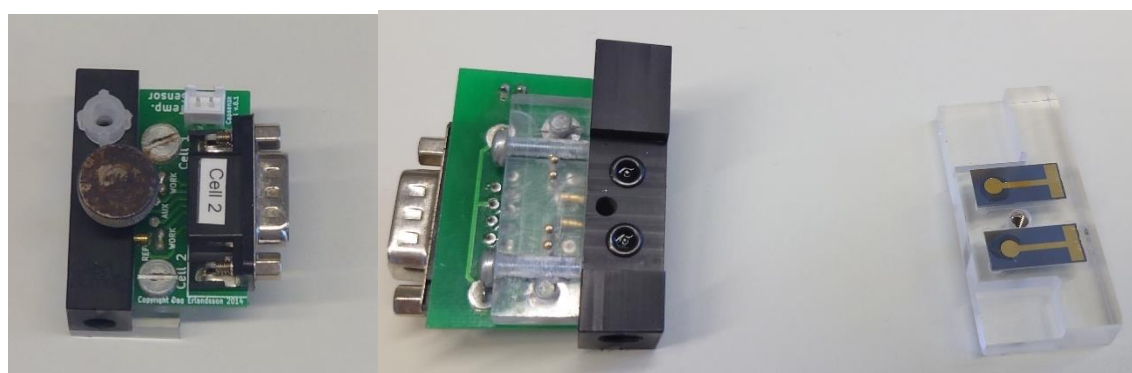


Figure 19: Left picture; assembled flow cell. Right picture: opened flow cell with working electrodes placed in their holders.

### 3.3.2 Detection methods

#### 3.3.2.1. Cyclic voltammetry

Cyclic voltammetry was performed on the Autolab PGSTAT302N with a three-electrode system. The working electrode was attached with a crocodile clamp. The auxiliary platinum electrode and the reference Ag/AgCl electrode was held in place with an electrode holder. The solution used was 10 mM  $K_3[Fe(CN)_6]$  in 1 M KCl. The endpoints were -300 mV and 800 mV, scan rate 100 mV/S exemplified in Figure 20. The scan was repeated three times when characterizing surfaces. When testing redox properties, the native buffer was used. Some measurements were performed in the flow cell with Pt electrodes with the same protocol.

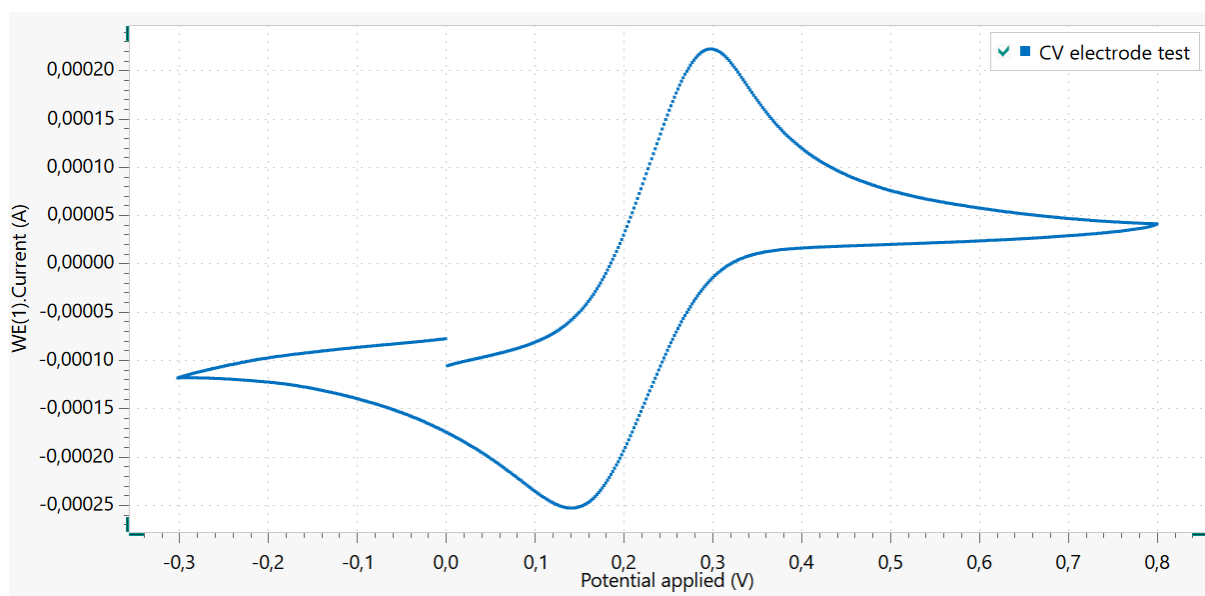


Figure 20: Typical cyclic voltammetry diagram.

#### 3.3.2.2. Amperometry

The initial studies of the system were performed on electrodes manufactured according to earlier protocol with the difference that the electrodes had three electropolymerization sweeps and that the attached antibody was of rabbit origin. The buffer used was mainly citrate buffer pH 5.5 adjusted with NaOH with different amounts of TMB,  $H_2O_2$  and swine anti-rabbit HRP antibody. TMB with  $H_2O_2$  in citric acid buffer is noted as detection buffer (DB).

The measurements were first conducted with the same setup as the cyclic voltammetry (Figure 18). The second iteration had manual injections into a flow-cell and the third system used a Lambda miniplus3 peristaltic pump and a manually controlled pneumatic injection valve with an injection loop of 50 or 100  $\mu$ l. An external Autolab PGSTAT302N was used for amperometric measurement. Both setups can be seen in Figure 13 and Figure 14.

The main measurements were performed on electrodes made according to earlier protocol with the difference that the electrodes had three electropolymerization sweeps and that the attached antibody was polyclonal rabbit anti-PTX3. The buffer used was citrate buffer pH 5.5 adjusted with NaOH with different amounts of TMB, H<sub>2</sub>O<sub>2</sub> and anti-PTX3 HRP Ab.

The flow part of the system was utilizing the Capsenze FIA system (Figure 21) controlled by the dedicated web-based software. The injection sequence was first performed with small blocks of commands, but the final program inject the sample pulse followed by a detection pulse. The program also regenerates the electrode with 0.25 mM pH 2.5 glycine.

The detection was performed in the described flow cell with the Autolab PGSTAT302N and used chronoamperometry with a fixed potential and measured the response in current.



*Figure 21: Overview of the final amperometric setup with attached FIA-system. FIA- system to the left, Autolab PGSTAT 302N I the middle and computer control computer to the right.*

### 3.3.2.3. Capacitive biosensor analysis

The first batch of electrodes were manufactured by using thermally deposited gold electrodes on silica wafers. Half of the electrodes was functionalized by using SAM and the other half was functionalized by electropolymerization (EP) of tyramine in 10 cycles. All according to earlier protocol, and protein G were immobilized on the surface. A second and third batch used 10 cycle tyramine activation and protein G. A part of the electrodes were capped with 1-dodecanethiol. The system used 10 mM Potassium phosphate pH 7.4 as buffer and glycine 0.25 mM pH 2.5-, or 0.1 mM pH 3 glycine for regeneration. As analyte a Swine anti-rabbit HRP antibody was used.

The small Capsenze biosensor system was used for all initial protein G based studies. Injection schemes from earlier projects were used to change parameters. The electrodes for the main experiment were manufactured according to the protocol for electropolymerization with 10 cycles and capped with 1-dodecanethiol see earlier protocol. Electropolymerized electrodes were used and polyclonal rabbit anti-PTX3 were attached with EDC-NHS chemistry using 5000X diluted anti-PTX3 antibody and subsequently further isolated with 1-dodecanethiol. The small Capsenze biosensor system was used for all capacitive studies, and injection parameters were changed by programming an injection scheme with accompanying software.

### 3.3.2.4. ELISA type analysis

To verify binding an ELISA type of protocol was used. The ELISA protocol used the analyte appropriate for the electrode and a secondary antibody with HRP. While washing with MQ and buffer in between the binding steps. Lastly, TMB was added to indicate if HRP was present before eluting.

## 4. Results and discussion

### 4.1 Characterization of electrodes

The CV results for respective states of the electrode. First a bare gold electrode that has been cleaned with piranha solution. Then a self-assembled monolayer and an electropolymerized electrode. These measurements was taken in a solution with 10 mM  $K_3[Fe(CN)_6]$  in 1 M KCl.

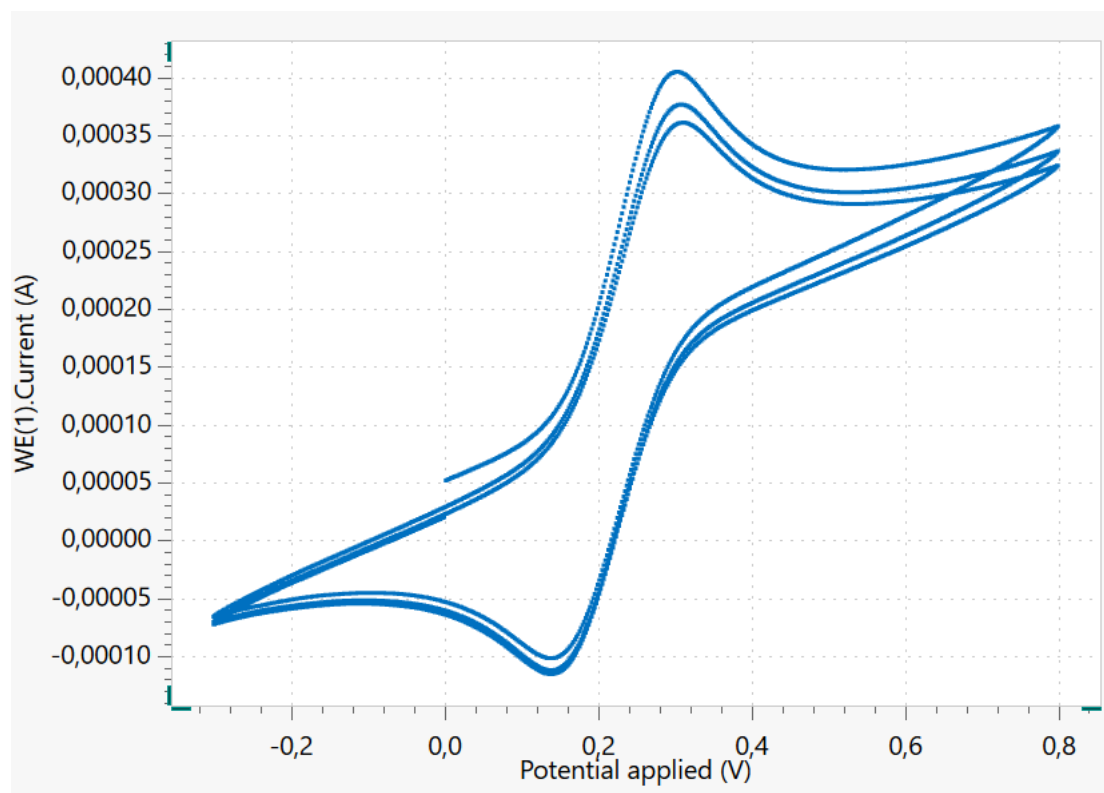


Figure 22: Cyclic voltammetry of piranha cleaned electrode in 10 mM  $K_3[Fe(CN)_6]$  in 1 M KCl.

The bare gold electrode has as expected good conductivity which can be seen by the large area in Figure 22.

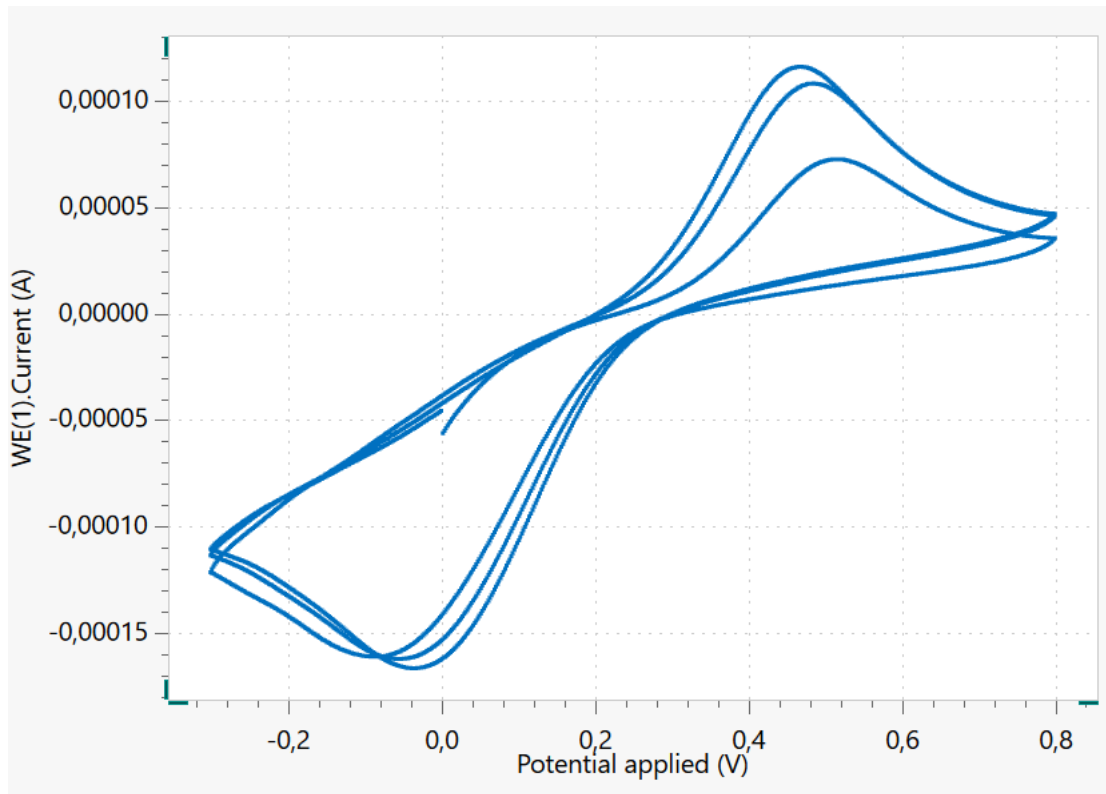


Figure 23: Cyclic voltammetry of self-assembled monolayer electrode in 10 mM  $K_3[Fe(CN)_6]$  in 1 M KCl

The activated electrode with a SAM (Figure 23) has decreased conductivity which is in line with current theory that adding layers isolates the surface.



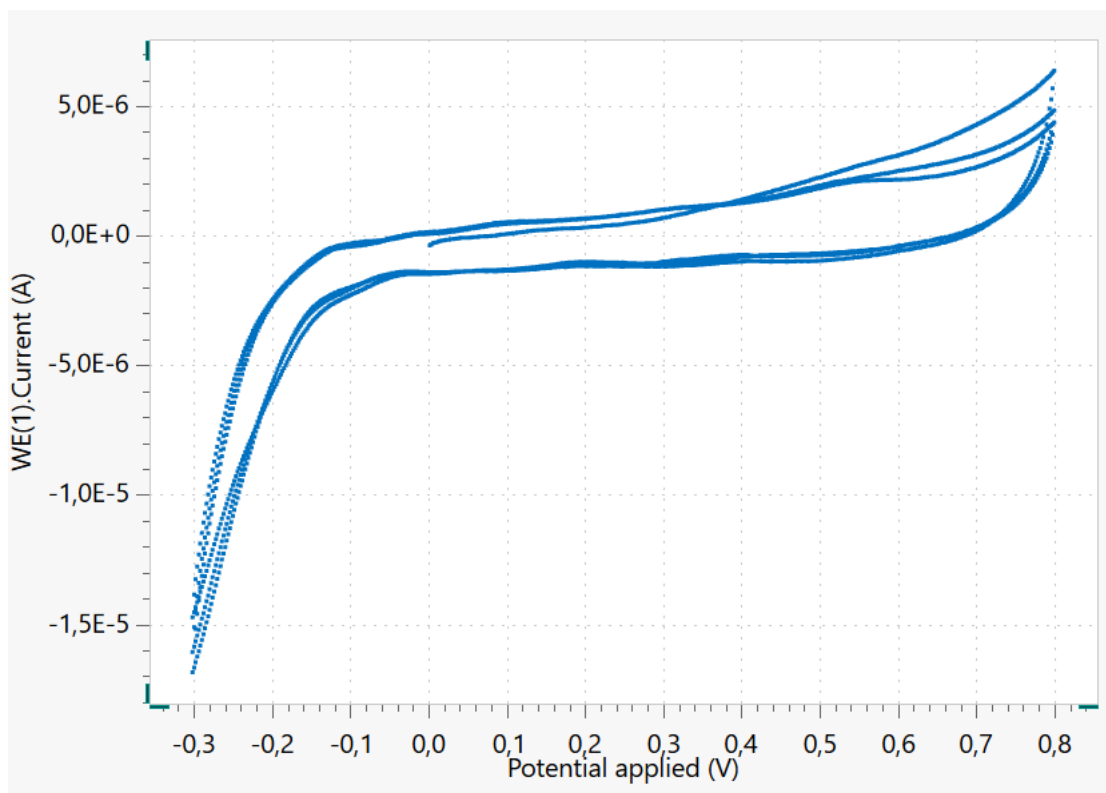


Figure 24: Cyclic voltammetry of electropolymerized electrode in 10 mM  $K_3[Fe(CN)_6]$  in 1 M KCl.

The electrode with 10 sweeps of electropolymerization (Figure 24) is more isolated than the SAM electrode. The electropolymerized electrode has theoretically a much thicker layer or rather multiple layers of polymers.

The second part of the surface characterization is the manufacturing of electropolymerized electrodes. This was done in 0.1 M tyramine and 0.3 M NaOH in methanol.

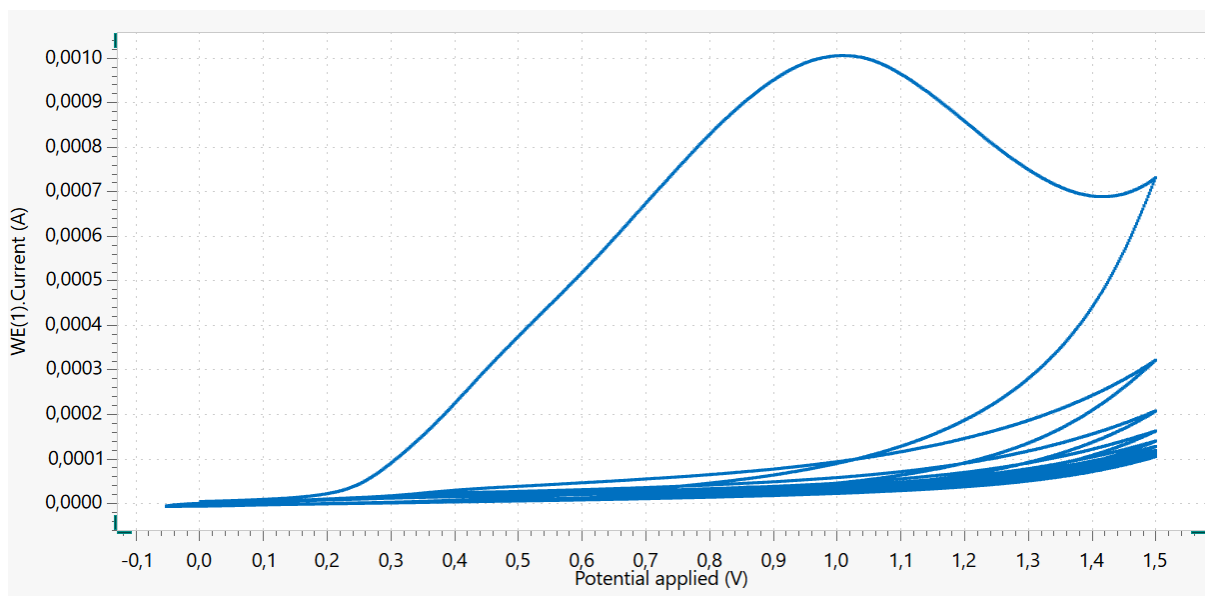


Figure 25: Electropolymerization 10 cycles. Gold electrode in 0.1 M tyramine and 0.3 M NaOH in methanol.

The first three CV sweeps results in the majority of the isolation, with diminishing returns towards ten sweeps (Figure 25).

## 4.2 Protein G model system

Protein G are used as biorecognition element. Swine anti-rabbit HRP are used as analyte, glycine 0.1 M pH 3 as regeneration and RB as carrier fluid.

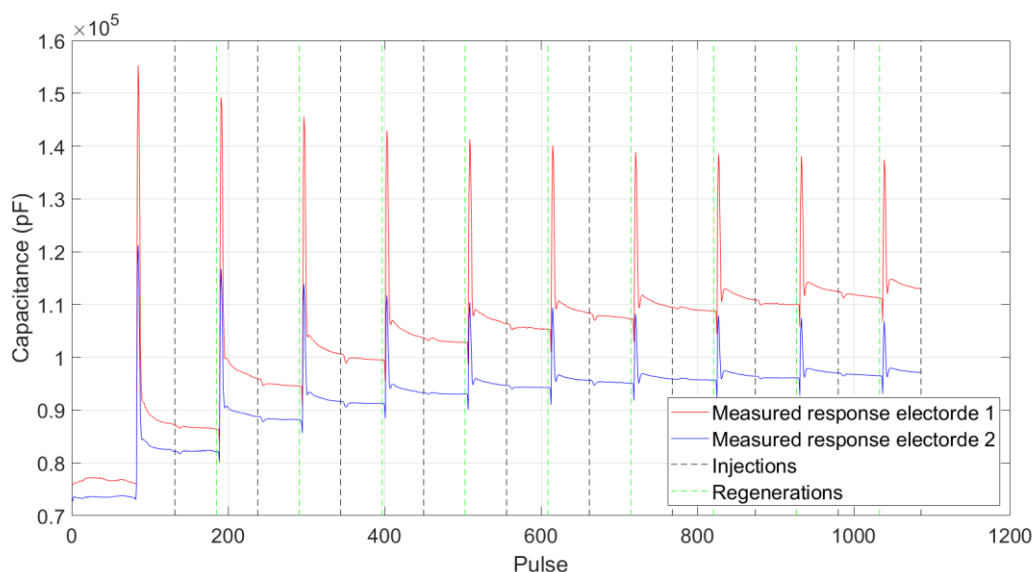


Figure 26: Overview of a typical run of capacitance measurements. This specific run: EP7A (red) EP10A (blue) three loops with three injections in each; One RB, then  $10^{-8}X$  swine anti-rabbit HRP Ab, then  $10^{-4}X$  swine anti-rabbit HRP Ab.

The run in Figure 26 was performed in the small Capsenze FIA system with integrated biosensor and was programmed into three loops where each loop had three injections. The first injection was RB, the second injection was low concentration of Ab ( $10^{-8}X$ ) and the third injection had high concentration of Ab ( $10^{-4}X$ ). The flow was  $1 \mu\text{l/s}$  and injection size of both regeneration with glycine and injection of sample was  $250 \mu\text{l}$ .

The interpretation of the capacitance measurements should consider the injection and regeneration and their respective delayed response on the electrode. The chronology is indicated by the pulse number on the x-axis. The delay is due to the volume in the tube between the valve and the flow-cell. The regeneration considerably affects the ionic environment since the glycine-HCl buffer has significantly higher ionic strength than RB inducing a major effect on the registered baseline (large peaks and dips). The expected outcome for a successful binding of an analyte is that the baseline capacitance is changed since it would add an additional layer on the surface of the working electrode.

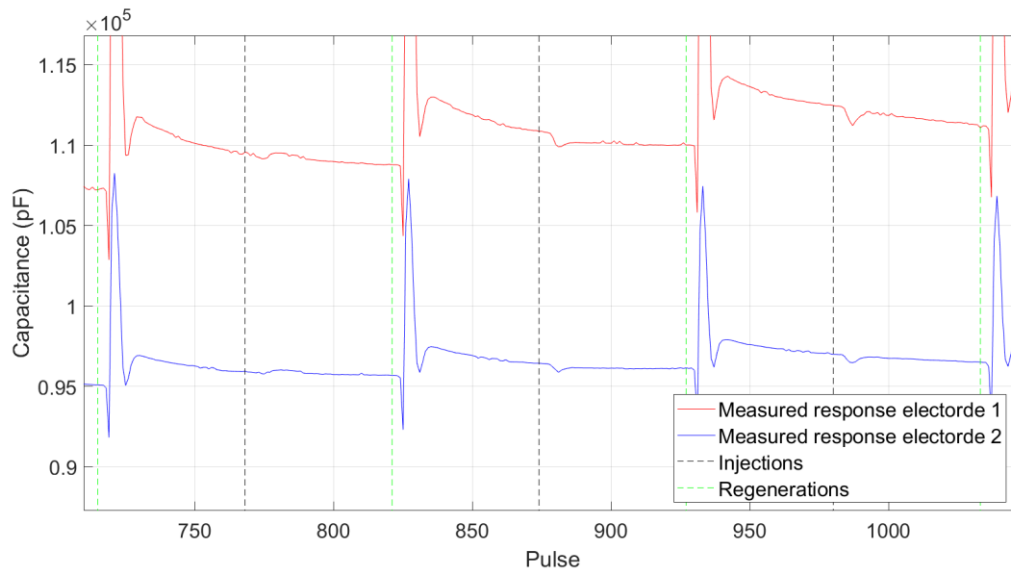


Figure 27: EP7A (red) EP10A (blue) loop three with injections from left: RB, then  $10^{-8}X$  swine anti-rabbit HRP Ab, then  $10^{-4}X$  swine anti-rabbit HRP Ab.

The left injection of RB in Figure 27 does not affect the baseline capacitance which is expected. The second injection of  $10^{-8}X$  swine anti-rabbit HRP does affect the baseline significantly. Unexpectedly, the higher concentration (third injection) to the right does not affect the baseline.

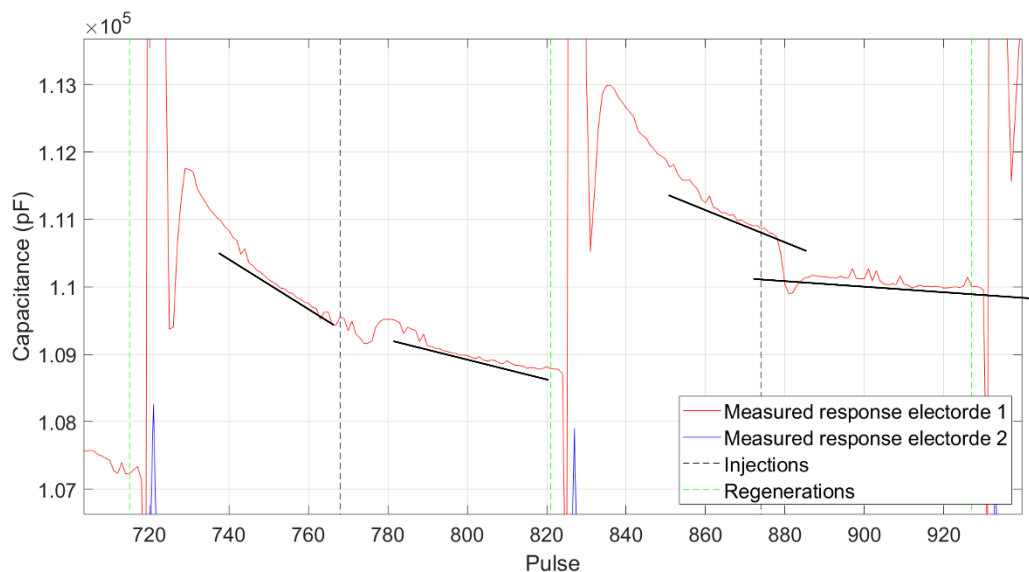


Figure 28: EP7A loop3 with comparison between blank injection(left) and  $10^{-8}X$  swine anti-rabbit HRP Ab (right). Baselines in black has been added to improve visualisation.

Figure 28 has clear indication of that the baseline change when injecting antibodies on the protein G electrode compared to when injecting RB. The electrode baseline stabilization, (pulses 885-925) is a clear indication that biomolecular binding occurs.

### 4.3 Capacitive measurements of PTX3

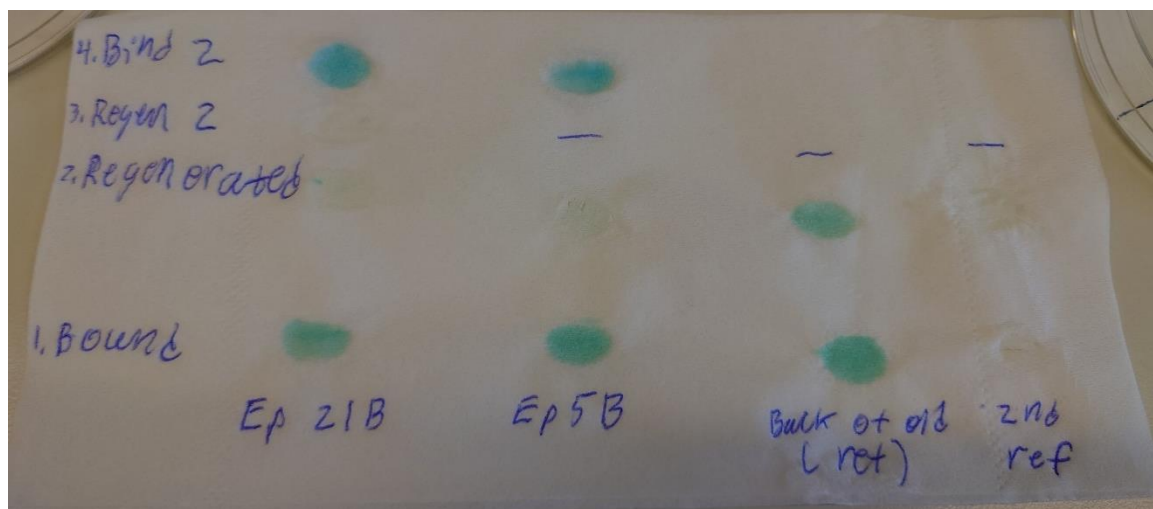


Figure 29: Test of electrode binding and regeneration with TMB. EP21B has been extensively used in the biosensor and EP5B has been used in the amperometric system. The test suggests that both has retained binding capacity for PTX3 + anti-PTX3 Ab HRP and that they can be regenerated with glycine.

The electrodes used in Figure 29 have been incubated with first PTX3 then anti-PTX3 HRP Ab and lastly TMB for the binding rows. For the regenerated rows the electrode has been washed with glycine.

Both EP21B and EP5B can bind anti-PTX3 HRP Ab after being used and seen on row one. Almost all HRP activity can be removed after using glycine indicating that the antibody can be removed seen on row two. The reference to the right (2<sup>nd</sup> ref) indicates that nothing activates or binds natively to an electrode that do not have immobilized anti-PTX3. The back of the old electrode seems to be not usable as a reference since TMB reacts with it despite of glycine washing.

These results show that the electrodes can bind the secondary antibody with HRP and that it can be removed with the glycine buffer. However, it does not confirm that the PTX3 can be removed with glycine.

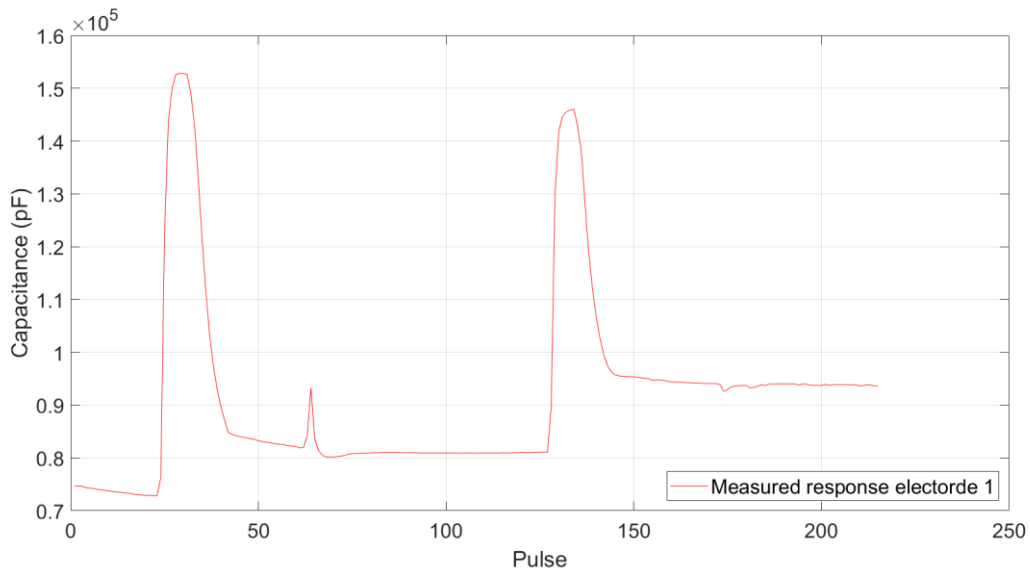


Figure 30:EP22B two regenerations and injections of PTX3 ( $10^{-3}X$ ). The injection on pulse 60 is the first injection PTX3 on electrode EP22B.

Injections of high concentration of PTX3 seen in Figure 30 does affect the electrode as seen by the spike around pulse 60 and the dip around pulse 170. The large peaks are regenerations with glycine.

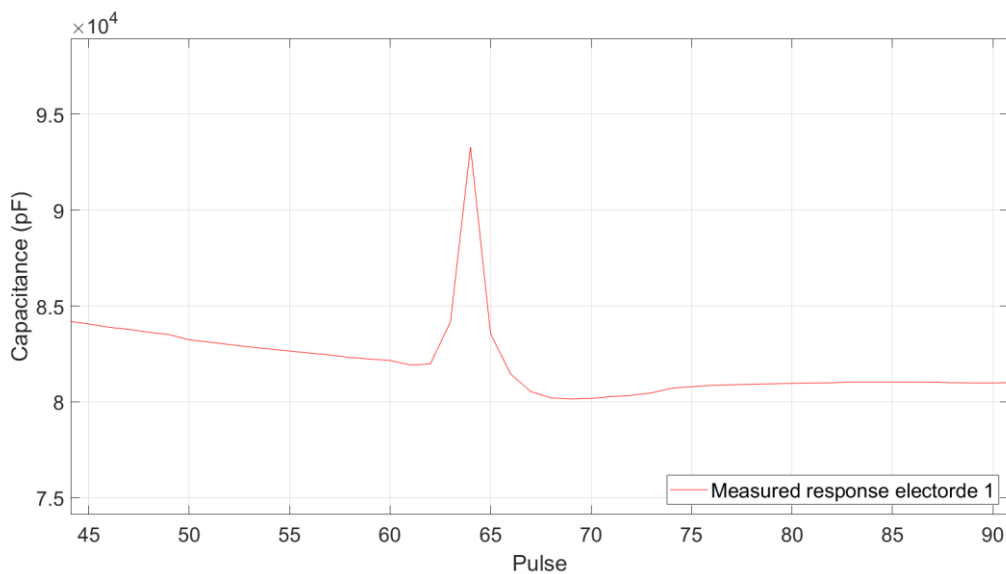


Figure 31:EP22B First injection of PTX3 ( $10^{-3}X$ ).

A more detailed picture in Figure 31 shows that the baseline does change, however it seems to recover and increase after a while.

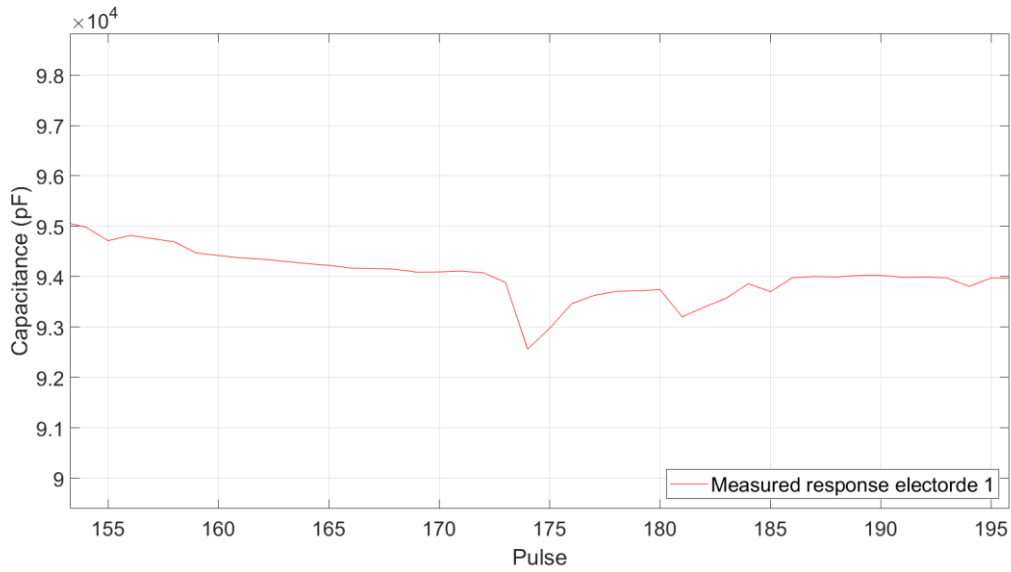


Figure 32: EP22B Second injection of PTX3 ( $10^{-3}X$ ).

The second injection ( Figure 32) of PTX3 with the same high concentration does not seem to change the baseline capacitance although the baseline seems more stable when it has recovered.

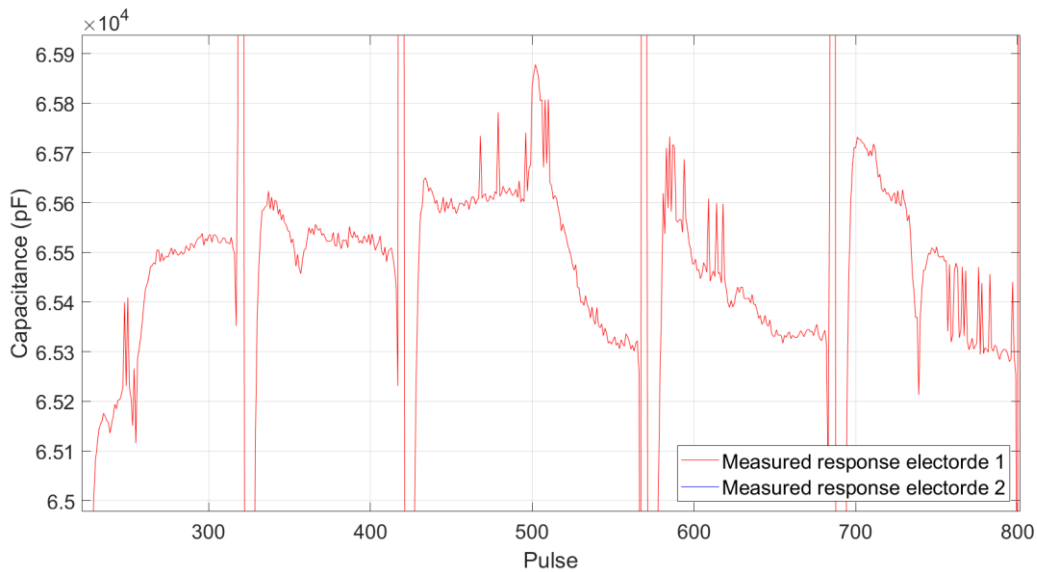


Figure 33: EP26B first injections. Injection starts; anti-PTX3 HRP Ab pulse 245 PTX3; pulse 340, pulse 493, pulse 612 (last anti-PTX3 HRP Ab pulse unknown). Anti-PTX3 HRP Ab  $10^{-3}X$ , PTX3  $10^{-14}X$ .

The first use of EP26B after first being regenerated to stabilize. The first injection to the left in Figure 33 is of anti-PTX3 HRP Ab. The subsequent three injections are of PTX3 in very low concentrations  $10^{-14}X$  and the last one to the right is of anti-PTX3 HRP Ab. The large peaks and dips in between each run are the result of electrode regeneration using glycine-HCl as dissociation buffer.

The results from this run are not undoubtably clear since the behaviour of the electrode is having some spikes. The main takeaways are that the first and last injection of anti-PTX3-HRP-Ab give very different responses on the electrode. Theoretically none of the should bind since no PTX3 should be on the surface, but for the first injection the electrode has never been exposed to PTX3 while for the last injection the surface has been regenerated after repeated PTX3 injections.

The three injections of PTX3 should theoretically give the same response since a FIA-system typically has very tight tolerances when it comes to injection volumes and timing. In this case they behave differently. The first injection seems to have a signal where the baseline shifts slightly.

The middle injection has an intentionally longer time to establish a pre injection baseline and then react very dramatically. The last injection gives a small dip but interestingly levels off towards a stable baseline.

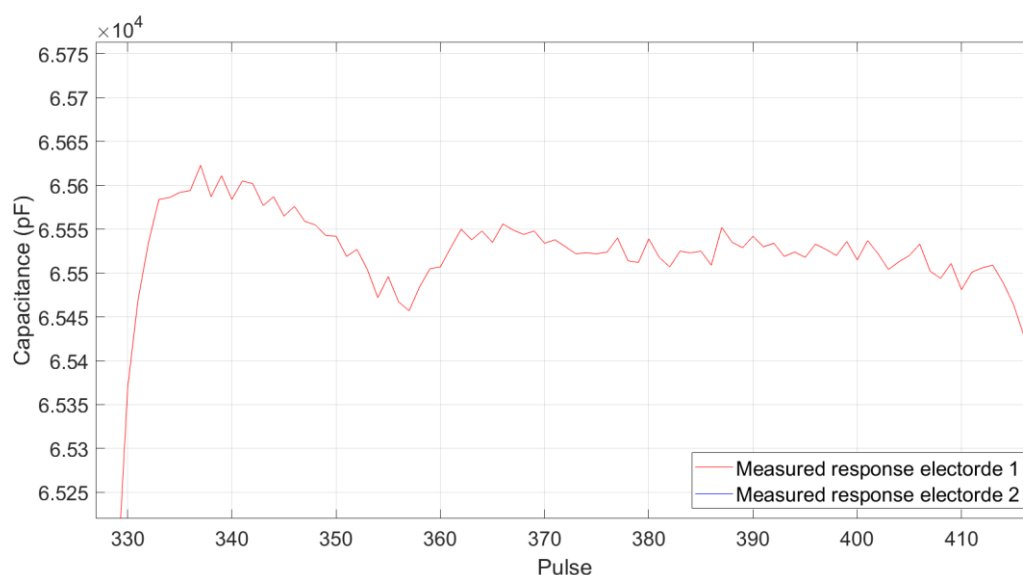


Figure 34: Zoom of EP26B first PTX3 contact  $10^{-14}X$  (injection at pulse 340).

A more detailed graph of the first PTX3 injection (Figure 34). The short baseline before injection takes place (pulses 332-340) is higher than the post-injection baseline (pulses 365-400). The stability of the post-injection baseline suggests that PTX3 might have bound even if the actual decrease in capacitance is low.

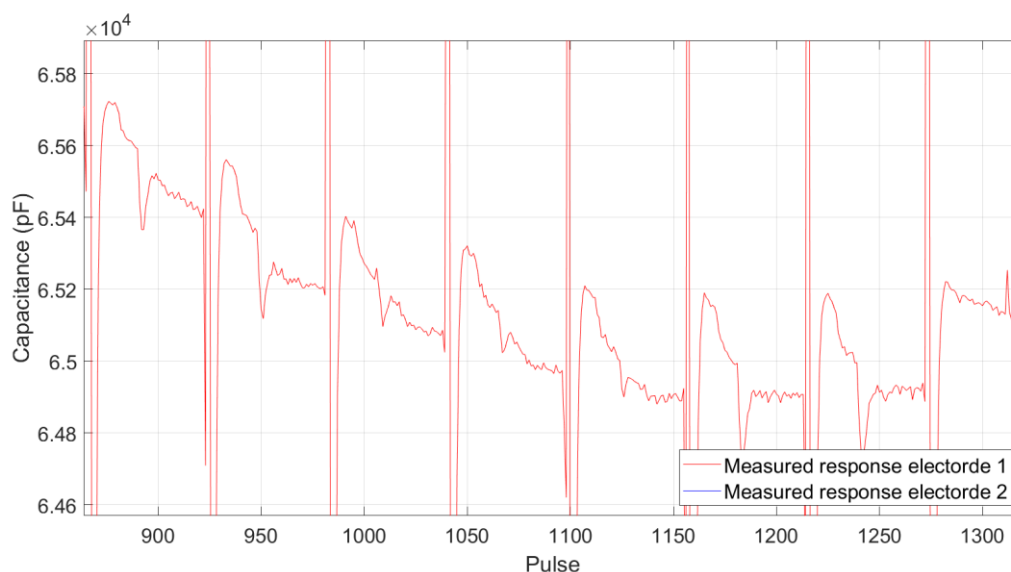


Figure 35: EP26B injection order from the left: 2 injections 50  $\mu$ l anti-PTX3-HRP-Ab ( $10^{-3}X$ ), 3 injections of 50  $\mu$ l PTX3  $10^{-14}X$ , 3 injections of 50  $\mu$ l RB, 2 injections of 50  $\mu$ l anti-PTX3-HRP-Ab ( $10^{-3}X$ ).

The drift of the capacitance is higher for the second run on EP26B as seen in Figure 35, making it harder to discern indications of binding. The two last injections of anti-PTX3 HRP Ab has a very clear patterns for binding with both a big drop in capacitance and a stabilizing effect. The only non-ideal conditions for these two measurements are that there is no clear stable baseline before injection.

The two first injections of anti-PTX3 HRP Ab has indications of binding, especially the second injection. For the three PTX3 injections the slope is too steep to make any certain conclusions.

There are two ways of interpreting these patterns, the easiest is to contribute the drift to a constant strive towards an ionic/electrical steady state for the electrode without any binding, since all three of the last injections have a similar post injection baseline. The counter argument to this is the rapid baseline stabilization of the two last injections of anti-PTX3 HRP Ab when compared to the measurements after the last regeneration. The slope is significantly less steep, meaning that the injection contributes to faster stabilization, presumably by binding.



## 4.4 Amperometry-preface

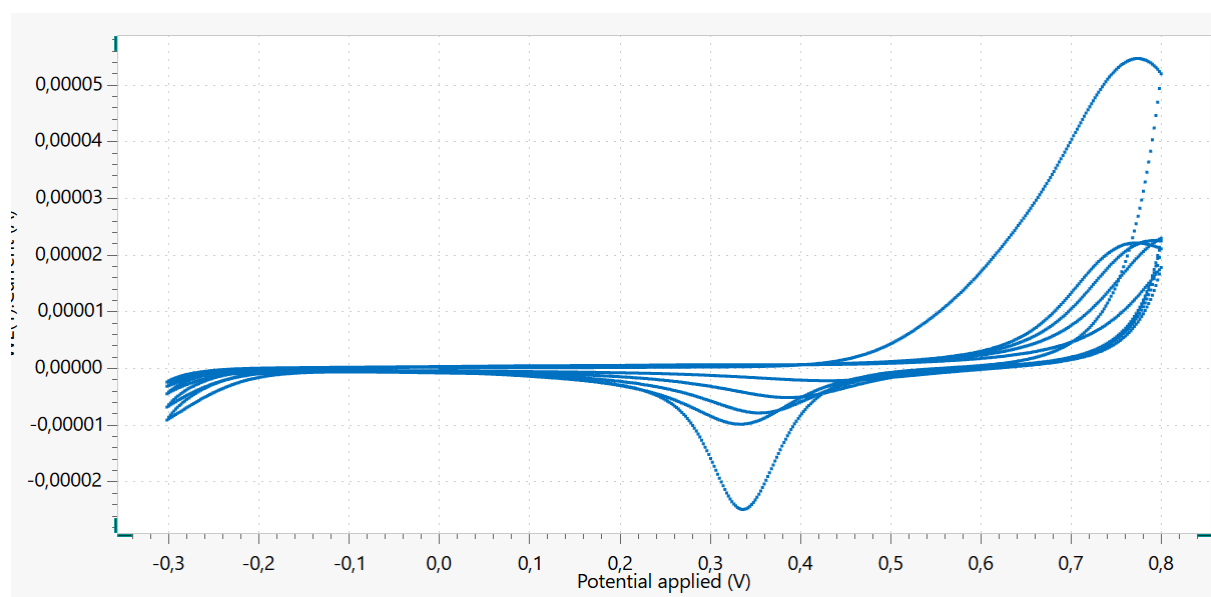


Figure 36: Cyclic voltammetry of bare gold electrode in Citric acid buffer pH 5.5 0.04 M, 5 sweeps. A diminishing oxidation peak at 0.32 V. measured in flow-cell with manual system.

Figure 36 shows the natural reduction and oxidation of citric acid buffer at pH 5.5 0.04 M. The reduction peaks at around 0.75 V and oxidation between 0.3 V and 0.4 V.

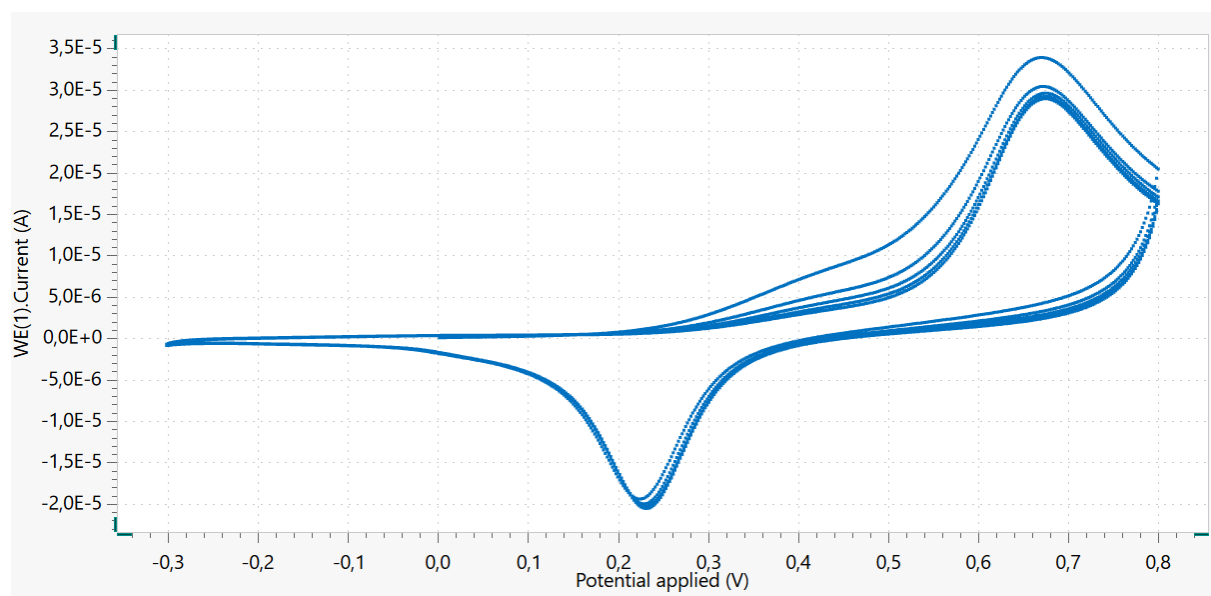


Figure 37: Cyclic voltammetry of bare gold electrode in Citric acid buffer pH 5.5 0.04 M with TMB and  $H_2O_2$ , 5 sweeps. A stable oxidation peak around 0.23 V measured in flow-cell with manual system.

The cyclic voltammetry spectrum (Figure 37) shows the potential of the reduction peak at 0.67 V and oxidation peak at 0.23 V for TMB in citric acid buffer 0.04 M at pH 5.5. The oxidation is repeatable and differs from the native oxidation of citric acid buffer. The repeatability is essential for decreasing variance in measurements using TMB for redox reactions.

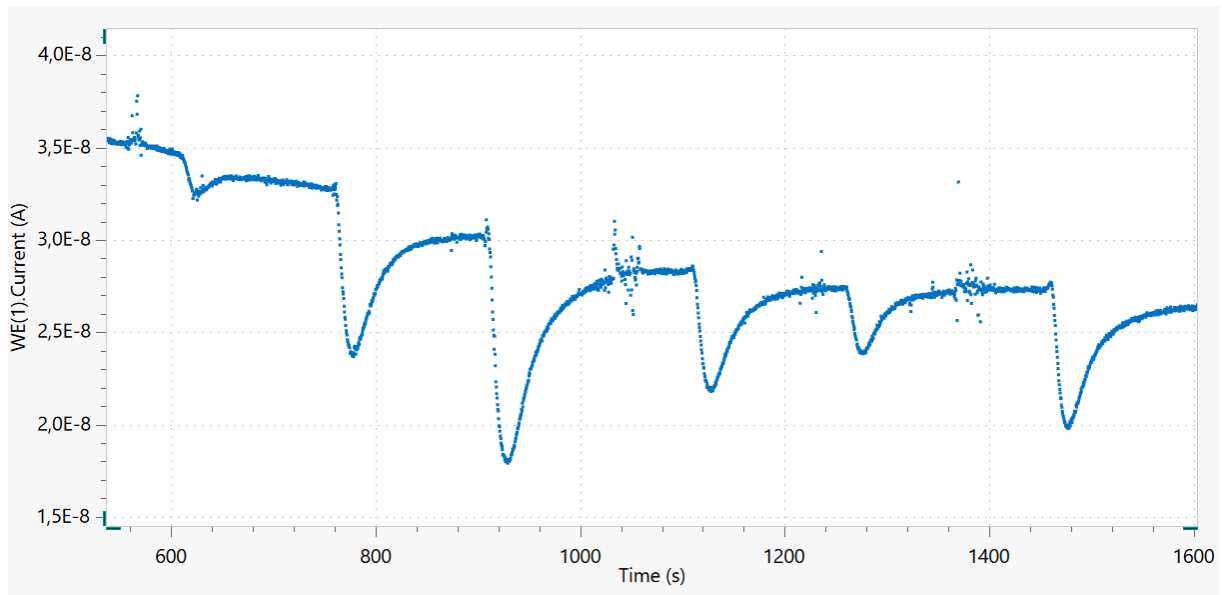


Figure 38: Electrode with immobilized rabbit antibodies at constant 0.25 V. Injections from left to right: DB, Low concentration of swine anti-rabbit HRP Ab, High concentration of swine anti-rabbit HRP Ab, GOAT Ab, DB extra low concentration of swine anti-rabbit HRP Ab. DB concentration: 40 ml citric acid buffer 0.04 M pH 5.5, 100  $\mu$ l 0.3%, H<sub>2</sub>O<sub>2</sub> 1  $\mu$ l TMB.

Injections of running buffer only result in a small response on the electrode (injection 1 and 5 Figure 38) while injections of swine anti-rabbit-antibody gives a response that is increasing with higher concentration (injection 2,3 and 4 Figure 38). An antibody that should not bind gives a response that is smaller than the lowest concentration of swine anti-rabbit. The HRP conjugated antibody should expectedly result in a change in current when HRP oxidizes TMB.

## 4.5 Amperometry PTX3

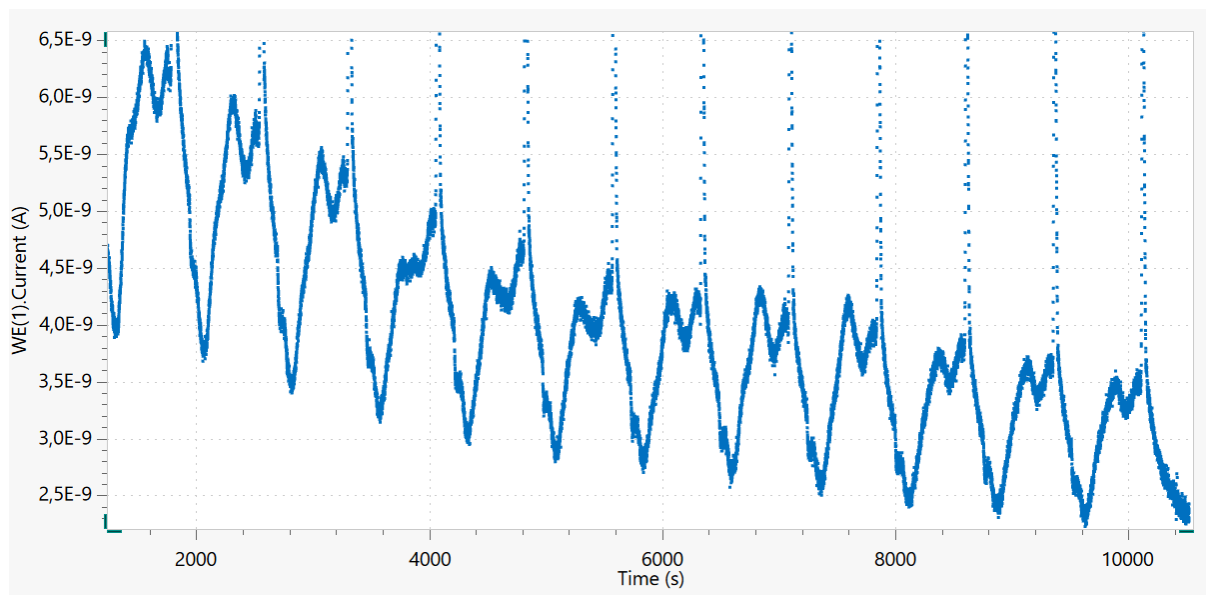


Figure 39: EPI2B 0.25 V Injection order from the left: three injections of 50 $\mu$ l blank sample + 50  $\mu$ l Anti-PTX3 HRP ( $10^{-4}X$ ), three injections of 50  $\mu$ l PTX3  $10^{-6}X$  + 50  $\mu$ l Anti-PTX3 HRP ( $10^{-4}X$ ), three injections of 50  $\mu$ l PTX3  $10^{-5}X$  + 50  $\mu$ l Anti-PTX3 HRP ( $10^{-4}X$ ), three injections of 50  $\mu$ l blank sample + 50  $\mu$ l Anti-PTX3 HRP ( $10^{-4}X$ ). Peak groups from each triplicate can be easily discerned.

The blank injections (running buffer) (injection 1-3 and 10-12) and PTX3 has different peak structures in Figure 39. There is a slight shift in the initial peak. The peak height is different between injections of PTX3  $10^{-5}X$  (injection 4-6) and PTX3  $10^{-6}X$  (injection 7-9). The current decreases over time meaning that the electrode is not in a steady state, the total height difference within each measurement also seem to be decreasing over time.

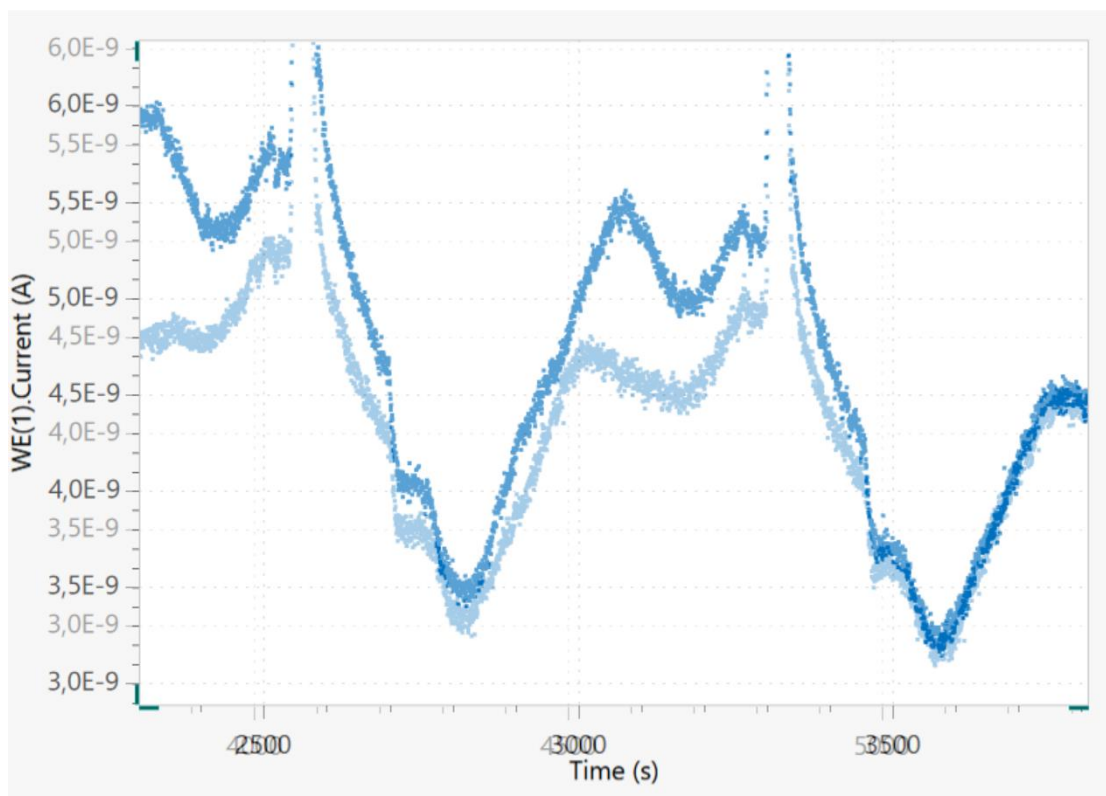


Figure 40: Difference in peak structure between blank injection (normal) and injection of PTX3 ( $10^{-4}X$ ) (faded).

The difference in peak structure in Figure 40 is not very apparent, only a slight shift between the blank injection and  $10^{-6}X$ . The difference seems to disappear when concentration increases according to Figure 39.

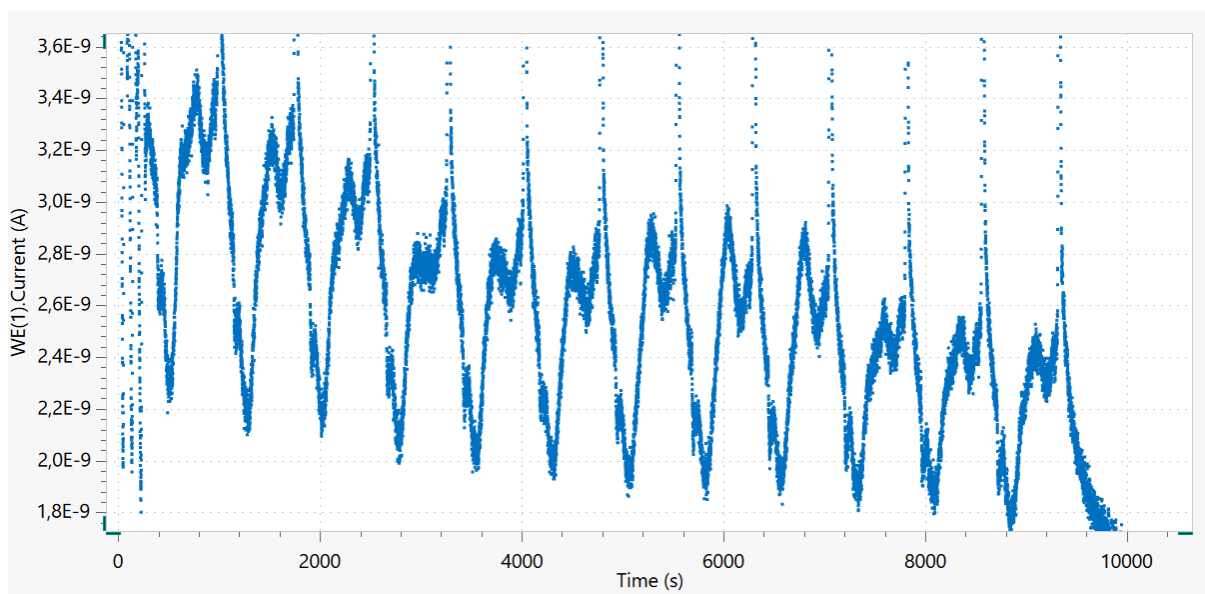


Figure 41: A second run with the same settings. EP12B 0.25 V Injection order from the left: three injections of 50  $\mu$ l blank sample + 50  $\mu$ l Anti-PTX3 HRP Ab( $10^{-4}X$ ), three injections of 50  $\mu$ l PTX3 ( $10^{-6}X$ ) + 50  $\mu$ l Anti-PTX3 HRP Ab ( $10^{-4}X$ ), 3 injections of 50  $\mu$ l PTX3  $10^{-5}X$  + 50  $\mu$ l Anti-PTX3 HRP ( $10^{-4}X$ ), three injections of 50  $\mu$ l blank sample + 50  $\mu$ l Anti-PTX3 HRP Ab( $10^{-4}X$ ). Peak groups from each triplicate can be easily discerned.

A second run (Figure 41) confirms the results.

## 4.6 Binding

The two systems used in this work produce initial evidence suggesting that biomolecular binding is taking place. The result in this report does however not show the whole picture for these systems and electrodes, there are several more results that are showing nothing or less successful results with similar and different configurations, some of these are presented in the appendix.

There are undoubtedly evidence that indicate that parts of both the amperometric and capacitive systems work. The utilized electrodes have a surface that has been polymerized to an extent according to Figure 24, the binding test (Figure 29) shows that the secondary anti-PTX3 antibody binds, and the model capacitive protein G system has a typical signal curve.

The model capacitive protein G system has clear evidence (Figure 28) that the system has signal upon injection of the target analyte, even with very low concentrations of the antibodies. The electrode can be regenerated and used several times. Too high concentrations however seem to overwhelm the sensor and does not give a good signal. A probable reason for this behaviour is that the dielectric layer formed during the current sweep is disrupted when too many molecules are crowding up at the surface. Evidently, this behaviour has been seen in several earlier applications on the capacitive sensor system.

The part that gives doubts in the binding test is whether the PTX3 is removed from the surface by glycine. Figure 34 suggests that PTX3 does bind to some extent, but later injections show no clear signs of binding in Figure 32, while the secondary antibody seems to bind. This pattern is even more evident in Figure 35. These indications points towards that the PTX3 binds but does not get released by regeneration. The PTX3 molecule as a monomer is large and has many possible places where an antibody could bind, but in the natural state it seems to be an octamer, increasing avidity. The glycine might not be enough. This stands in contrast to the results from the protein G based system where repeatable behaviour with stabilizing baselines indicate binding of antibodies.

However, if the permanent binding of PTX3 was true, the same behaviour should be seen in the amperometric system. But according to Figure 39 and Figure 40 the behaviour of these measurements are very repeatable, not indicating any permanent binding of PTX3. The systems differ in two main ways, the buffer and electrical potential applied. The amperometric system has a citric acid buffer pH 5.5 0.04 M, TMB and H<sub>2</sub>O<sub>2</sub> and a constant voltage of 0.25 V, while the capacitive system has potassium phosphate buffer pH7.4 and no constant voltage applied. It would not be impossible for the applied voltage, pH, and different ions to change condition enough to give the two systems different binding characteristics.

The other options are that the amperometric system does not truly have a binding or a very weak binding, have ionic disruptions, or that the measurement is done in a manner that misses the TMB oxidation. Some of these arguments are however weak since both the protein G and PTX3 systems shows signal. Especially the protein G systems even shows that there might be signal correlation with concentration that is separable from interfering compounds.

## 4.7 Comparison of systems

If the systems truly have binding and signal for the current setups, the comparison between them and other available systems becomes relevant. The capacitive system would according to the results detect approximately 10<sup>-20</sup> M while the amperometric system would detect approximately 10<sup>-12</sup> M PTX3. The capacitive system could then be classified as an ultra-sensitive system that has among the best sensitivity available for these types of systems. The amperometric system would be in line with some ELISA kits for PTX3 while the capacitive system would surpass all current available systems in sensitivity that uses DPV and SPR. The amperometric system is however probably cheaper to introduce and scale than the capacitive. It also has a much higher throughput and low manual labour compared to ELISA.

## 4.8 Conclusion

This work has explored a capacitive and an amperometric analytical system for analysis of PTX3. The capacitive system showed excellent sensitivity detecting PTX3 at concentrations of 10<sup>-20</sup> M in buffer. The amperometric system could detect concentrations of 10<sup>-12</sup> M PTX3. Both systems should in this stage be seen as viable for future development of a more specialized system for clinical use.

## **5. Future perspectives**

In this study, it was possible to see a clear signal for both analytical systems. However, much work remains to achieve a validated method to be used in e.g., clinical analysis. Hence, this work should be seen as an initial prospect for the feasibility of the amperometric and capacitive measurement for PTX3 analysis. For both analytical techniques there are certainly room for improvement of protocols and parameters. The next step would be to establish calibration curves and move towards blood as a sample matrix and test interference for closely related proteins such as CRP.

## 6. References

1. Saylan Y, Erdem Ö, Ünal S, Denizli A. An Alternative Medical Diagnosis Method: Biosensors for Virus Detection. *Biosensors*. 2019;9(2):65.
2. Bohunicky B, Mousa SA. Biosensors: the new wave in cancer diagnosis. *Nanotechnology, Science and Applications*. 2011;4:1-10.
3. Mellhammar L. Vårdprogram sepsis-tidig identifiering och behandling vid samhällsförvärvad sepsis hos vuxna. In: skåne R, editor. 2023.
4. Eriksson N. Blododling: Unilabs; 2022 [updated 2022-09-27. Available from: <https://anvisningar.se/Anvisningar/Klinisk-mikrobiologi/B/Blododling/>.
5. Duncan CF, Youngstein T, Kirrane MD, Lonsdale DO. Diagnostic Challenges in Sepsis. *Current Infectious Disease Reports*. 2021;23(12):22.
6. Singer M, Deutschman CS, Seymour CW, Shankar-Hari M, Annane D, Bauer M, et al. The Third International Consensus Definitions for Sepsis and Septic Shock (Sepsis-3). *Jama*. 2016;315(8):801-10.
7. Barichello T, Generoso JS, Singer M, Dal-Pizzol F. Biomarkers for sepsis: more than just fever and leukocytosis—a narrative review. *Critical Care*. 2022;26(1):14.
8. Davoudian S, Piovani D, Desai A, Mapelli SN, Leone R, Sironi M, et al. A cytokine/PTX3 prognostic index as a predictor of mortality in sepsis. *Frontiers in Immunology*. 2022;13.
9. Pfaller MA, Wolk DM, Lowery TJ. T2MR and T2Candida: novel technology for the rapid diagnosis of candidemia and invasive candidiasis. *Future Microbiology*. 2016;11(1):103-17.
10. Song J, Moon S, Park DW, Cho H-J, Kim JY, Park J, et al. Biomarker combination and SOFA score for the prediction of mortality in sepsis and septic shock: A prospective observational study according to the Sepsis-3 definitions. *Medicine*. 2020;99(22):e20495.
11. Chen H, Li T, Yan S, Liu M, Liu K, Zhang H, et al. Pentraxin-3 Is a Strong Biomarker of Sepsis Severity Identification and Predictor of 90-Day Mortality in Intensive Care Units via Sepsis 3.0 Definitions. *Diagnostics (Basel)*. 2021;11(10).
12. Zhang Q, Wu J, Niu W, Xue J. Nanocomposites prepared from gold nanowires and multiwalled carbon nanotubes for non-enzymatic sensitive bioelectrochemical detection of pentraxin-3 in human serum. *Ionics*. 2021;27:1-8.
13. Canovi M, Lucchetti J, Stravalaci M, Valentino S, Bottazzi B, Salmons M, et al. A New Surface Plasmon Resonance-Based Immunoassay for Rapid, Reproducible and Sensitive Quantification of Pentraxin-3 in Human Plasma. *Sensors*. 2014;14(6):10864-75.
14. Höfs S, Hülögü D, Bennet F, Carl P, Flemig S, Schmid T, et al. Electrochemical Immunomagnetic Ochratoxin A Sensing: Steps Forward in the Application of 3,3',5,5'-Tetramethylbenzidine in Amperometric Assays. *ChemElectroChem*. 2021;8(13):2597-606.
15. Erdem A, Senturk H, Yildiz E, Maral M. Amperometric immunosensor developed for sensitive detection of SARS-CoV-2 spike S1 protein in combined with portable device. *Talanta*. 2022;244:123422.
16. Teeparuksapun K. Capacitive Biosensor - A Tool for Ultrasensitive Analysis : Application in Clinical Analysis and Process Monitoring [phdthesis]: Lund University (Media-Tryck); 2013.
17. Porte R, Davoudian S, Asgari F, Parente R, Mantovani A, Garlanda C, et al. The Long Pentraxin PTX3 as a Humoral Innate Immunity Functional Player and Biomarker of Infections and Sepsis. *Frontiers in Immunology*. 2019;10.
18. Yamasaki K, Kurimura M, Kasai T, Sagara M, Kodama T, Inoue K. Determination of physiological plasma pentraxin 3 (PTX3) levels in healthy populations. *Clinical Chemistry and Laboratory Medicine*. 2009;47(4):471-7.
19. Noone DP, Dijkstra DJ, van der Klugt TT, van Veelen PA, de Ru AH, Hensbergen PJ, et al. PTX3 structure determination using a hybrid cryoelectron microscopy and AlphaFold approach offers insights into ligand binding and complement activation. *Proceedings of the National Academy of Sciences*. 2022;119(33):e2208144119.



20. Pan HM, Gonuguntla S, Li S, Trau D. 3.33 Conjugated Polymers for Biosensor Devices☆. In: Ducheyne P, editor. *Comprehensive Biomaterials II*. Oxford: Elsevier; 2017. p. 716-54.
21. . Lund university: Martin Hedström; 2023.
22. Chapter 2 FIA Principles and Theories. In: Karlberg B, Pacey GE, editors. *Techniques and Instrumentation in Analytical Chemistry*. 10: Elsevier; 1989. p. 6-28.
23. Ruiz-Medina A. Flow Analysis | Flow Injection Analysis: Clinical and Pharmaceutical Applications. In: Worsfold P, Poole C, Townshend A, Miró M, editors. *Encyclopedia of Analytical Science (Third Edition)*. Oxford: Academic Press; 2019. p. 145-53.
24. Kenneth Murphy CW. *Janeway's immunobiology*. 9 ed. New York, NY: Garland Science/Taylor & Francis Group; 2016. 904 p.
25. Paimard G, Ghasali E, Baeza M. Screen-Printed Electrodes: Fabrication, Modification, and Biosensing Applications. *Chemosensors*. 2023;11(2):113.
26. DropSens M. SCREEN-PRINTED ELECTRODES (SPEs). Dropsense.com: Dropsense.
27. Vashist SK, Luong JHT. Chapter 2 - Antibody Immobilization and Surface Functionalization Chemistries for Immunodiagnosics. In: Vashist SK, Luong JHT, editors. *Handbook of Immunoassay Technologies: Academic Press*; 2018. p. 19-46.
28. scientific TF. Thermo Fisher scientific: Thermo Fisher scientific.
29. Hermanson GT. Chapter 4 - Zero-Length Crosslinkers. In: Hermanson GT, editor. *Bioconjugate Techniques (Third Edition)*. Boston: Academic Press; 2013. p. 259-73.
30. Nikkhah M, Karami S, Khatami SH, Taheri-Anganeh M, Savardashtaki A, Mahmoodzadeh A, et al. Review of electrochemical and optical biosensors for testosterone measurement. *Biotechnology and Applied Biochemistry*. 2023;70(1):318-29.
31. Forster RJ, Walsh D, Adamson K, Spain E. Voltammetry | Overview☆. In: Worsfold P, Poole C, Townshend A, Miró M, editors. *Encyclopedia of Analytical Science (Third Edition)*. Oxford: Academic Press; 2019. p. 209-17.
32. Elgrishi N, Rountree KJ, McCarthy BD, Rountree ES, Eisenhart TT, Dempsey JL. A Practical Beginner's Guide to Cyclic Voltammetry. *Journal of Chemical Education*. 2018;95(2):197-206.
33. Amine A, Mohammadi H. Amperometry☆. In: Worsfold P, Poole C, Townshend A, Miró M, editors. *Encyclopedia of Analytical Science (Third Edition)*. Oxford: Academic Press; 2019. p. 85-98.
34. Д.Ильин. Electric double-layer (BMD model) NT-int. Wikimedia commons: Wikimedia commons; 2021. p. Electric double-layer (BMD model) No text 1.IHP (Inner Helmholtz Layer) 2.OHP (Outer Helmholtz Layer) 3.Diffusion layer 4.Solvated ions 5.Peculiar adsorptive ions 6.Solvent molecule.
35. Mahadhy A. Development of an Ultrasensitive Capacitive DNA-sensor: A promising tool towards microbial diagnostics: Lund University; 2015.
36. Erlandsson D, Teeparuksapun K, Mattiasson B, Hedström M. Automated flow-injection immunosensor based on current pulse capacitive measurements. *Sensors and Actuators B: Chemical*. 2014;190:295-304.
37. technologies i. HRP Redox Reaction Driven TMB Color Development: immunochemistry technologies; [Available from: <https://www.immunochemistry.com/pages/hrp-redox-reaction-driven-tmb-color-development>].

## 7. Appendix

### 7.1 Electrode overview

Table A: Overview of electrodes used in the later part of the experiments.

Electrode	Activation		Biorecognition element	Immobilization concentration
EP1A	Electropolymerization cycles	10	Protein G	$6.5 \cdot 10^{-4}$ g/l
EP2A	Electropolymerization cycles	10	Ab rabbit	$5.66 \cdot 10^{-4}$ g/l
EP3A	Electropolymerization cycles	10	None	
EP4A	Electropolymerization cycles	10	Protein G	$6.5 \cdot 10^{-4}$ g/l
EP5A	Electropolymerization cycles	10	Ab rabbit	$5.66 \cdot 10^{-4}$ g/l
EP6A	Electropolymerization cycles	10	None	
EP7A	Electropolymerization cycles	10	Protein G	$6.5 \cdot 10^{-4}$ g/l
EP8A	Electropolymerization cycles	10	Ab rabbit	$5.66 \cdot 10^{-4}$ g/l
EP9A	Electropolymerization cycles	10	None	
EP10A	Electropolymerization cycles	10	Protein G	$6.5 \cdot 10^{-4}$ g/l
EP11A	Electropolymerization cycles	10	Ab rabbit	$6.5 \cdot 10^{-4}$ g/l
EP1B	Electropolymerization cycles	3	Anti-PTX3	5000X
EP2B	Electropolymerization cycles	3	Anti-PTX3	5000X
EP3B	Electropolymerization cycles	3	Anti-PTX3	5000X
EP4B	Electropolymerization cycles	3	Anti-PTX3	5000X
EP5B	Electropolymerization cycles	3	Anti-PTX3	5000X
EP6B	Electropolymerization cycles	3	Anti-PTX3	5000X
EP7B	Electropolymerization cycles	3	Anti-PTX3	5000X

Electrode	Activation		Biorecognition element	Immobilization concentration
EP8B	Electropolymerization cycles	3	Anti-PTX3	5000X
EP9B	Electropolymerization cycles	3	Anti-PTX3	5000X
EP10B	Electropolymerization cycles	3	Anti-PTX3	5000X
EP11B	Electropolymerization cycles	3	Anti-PTX3	5000X
EP12B	Electropolymerization cycles	3	Anti-PTX3	5000X
EP13B	Electropolymerization cycles	3	Unused	
EP13B BISS	Electropolymerization cycles	3	Unused	
EP14B	Electropolymerization cycles	3	Unused	
EP15B	Electropolymerization cycles	3	Unused	
EP16B	Electropolymerization cycles	3	Unused	
EP17B	Electropolymerization cycles	3	Unused	
EP18B	Electropolymerization cycles	3	Unused	
EP19B	Electropolymerization cycles	3	Unused	
EP20B	Electropolymerization cycles	3	Unused	
EP21B	Electropolymerization cycles	10	Anti-PTX3	5000X
EP22B	Electropolymerization cycles	10	Anti-PTX3	5000X
EP23B	Electropolymerization cycles	10	Anti-PTX3	5000X
EP24B	Electropolymerization cycles	10	Anti-PTX3	5000X
EP25B	Electropolymerization cycles	10	Anti-PTX3	5000X
EP26B	Electropolymerization cycles	10	Anti-PTX3	5000X
EP27B	Electropolymerization cycles	10	Anti-PTX3	5000X
EP28B	Electropolymerization cycles	10	Anti-PTX3	5000X
EP29B	Electropolymerization cycles	10	Unused	

Electrode	Activation		Biorecognition element	Immobilization concentration
EP30B	Electropolymerization cycles	10	Unused	
EP31B	Electropolymerization cycles	10	Unused	
EP32B	Electropolymerization cycles	10	Unused	
EP33B	Electropolymerization cycles	10	Unused	
EP34B	Electropolymerization cycles	10	Unused	
EP35B	Electropolymerization cycles	10	Unused	
EP36B	Electropolymerization cycles	10	Unused	
EP37B	Electropolymerization cycles	10	Unused	
EP38B	Electropolymerization cycles	10	Unused	
EP39B	Electropolymerization cycles	10	Unused	

## 7.2 Protocols

### 7.2.1 Protocol self-assembling monolayer

1. Treat surface with piranha solution 1:3 (10min)
2. Flush with ethanol
3. Immediately put electrode in  $\alpha$ -lipoic acid (2% in ethanol) and wait 24h
4. Rinse with ethanol, dry with N<sub>2</sub> rinse with MQ then dry with N<sub>2</sub>
5. Mix frozen EDC (0.4 M) and NHS (0.1 M) 1:1 and immediately activate the surface with EDC/NHS (1h RT)
6. Rinse with RB, dry with N<sub>2</sub>
7. Place freshly prepared ligand solution on the electrode (ON or OW in fridge with extra moisture)
8. Rinse with RB, dry with N<sub>2</sub>, rinse with ethanol
9. Immerse in 1-dodecanethiol (10 mM in ethanol)
10. Rinse with ethanol, dry with N<sub>2</sub> Rinse with RB
11. Store in RB in fridge

### 7.2.2 Protocol electropolymerization

1. Treat surface with piranha solution 1:3 (10 min)
2. Rinse with MQ
3. CV 0-1.5 V (vs Ag/AgCl) scan rate 50 mV/s (10 scans) in 10 methanol (100 mM tyramine, 300 mM NaOH)
4. Rinse with MQ and RB (K-PB pH 7.4) dry with N<sub>2</sub>.
5. Mix frozen EDC (0.4 M) and NHS (0.1 M) 1:1 and immediately activate the surface with EDC/NHS (1h RT)
6. Rinse with RB, dry with N<sub>2</sub>
7. Place freshly prepared ligand solution on the electrode (ON or OW in fridge with extra moisture)
8. Rinse with RB, dry with N<sub>2</sub>, rinse with ethanol
9. Immerse in 1-dodecanethiol (10 mM in ethanol)
10. Rinse with ethanol, dry with N<sub>2</sub> Rinse with RB
11. Store in RB in fridge

## 7.3 Figures

Examples of runs without good signal.

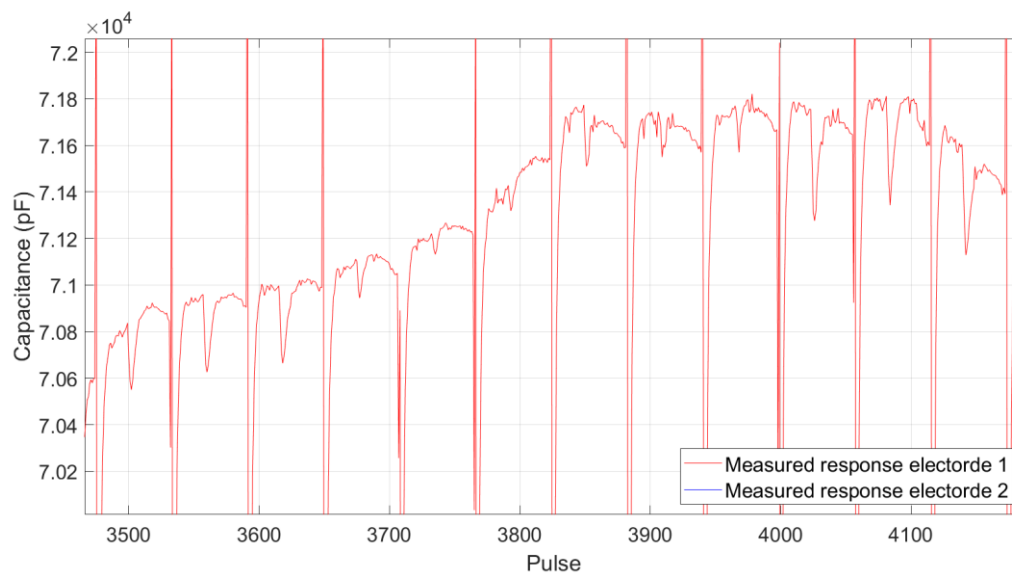


Figure A: EP26B P3365run (3HRP3PTX3RB3HRP) Injection order from the left: three injections 50  $\mu$ l Anti-PTX3 HRP ( $10^{-4}X$ ), three injections of 50 $\mu$ l PTX3  $10^{-14}X$ , three injections of 50 $\mu$ l RB, three injections of 50  $\mu$ l Anti-PTX3 HRP ( $10^{-4}X$ ). Peak groups from each triplicate can be easily discerned.

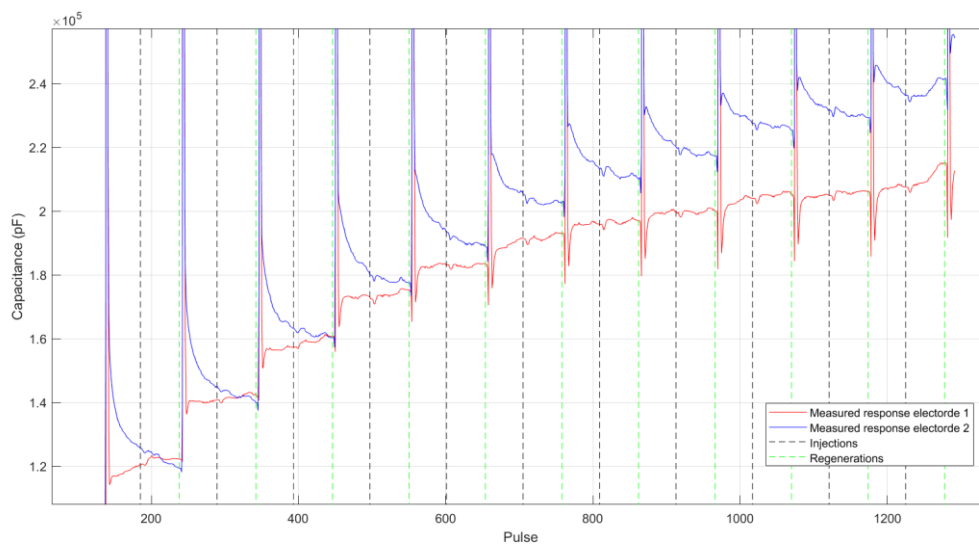


Figure B: Typical capacitance run without signal.

## 7.4 MATLAB scripts

Script for reading data from the files produced by the small Capsenze capacitance instrument.

The script below reads files with two electrodes. There are two other variants, one for reading one electrode and one for reading data when injection is done by another system.

```
% close all

%% NY variant av import
%import cap
filename = 'C:\Users\Dell\OneDrive - Lund University\Examensarbete Viktor\Data\Runs
malin4\capsenze_068\cap.txt';
delimiter = '\t'; % assuming that the data is tab-delimited
formatSpec = repmat('%f', 1, 12); % assuming that there are 12 columns of data
opts = detectImportOptions(filename, 'Delimiter', delimiter);
opts.DataLines = 1; % read the first line to get the number of variables
CAP = readtable(filename, opts);
%import log
filename = 'C:\Users\Dell\OneDrive - Lund University\Examensarbete Viktor\Data\Runs
malin4\capsenze_068\log.txt';
delimiter = {'|', '('}; % assuming that the data is tab-delimited
formatSpec = repmat('%f', 1, 1); % assuming that there are 12 columns of data
opts = detectImportOptions(filename, 'Delimiter', delimiter);
opts.DataLines = 1; % read the first line to get the number of variables
LOG = readtable(filename, opts);

%% NY Uppdelning av data

%formatera om log för sökbarhet
LOG = table2cell(LOG);

LOGSEARCH = LOG(:,4);

%formaterar om cap för plottning
CAP=CAP(:,1:11);

CAP= rmmissing(CAP);
CAPB = sortrows(CAP,2);

CAPC= table2cell(CAPB);
%%
si= size(CAPC);
rows=si(1)./2;

series0= CAPB(1:rows,:);
series1= CAPB((rows+1):end,:);

%% Ny hitta injektioner
%Index = find(contains(log,'Standard injection done.)); %stämmer med
%injektioner för YL sequential
Index = find(contains(LOGSEARCH,'Regenerate done'));% stämmer med portinject

text= LOG(Index,2);
text=string(text); %%%%%%%%%%%%%%% får ut rätt strings fortsätt här

% Use regexp to extract the numbers
numbers = regexp(text, '\d+', 'match');

% Convert the cell array of strings to a numeric array
numbers = cellfun(@str2double,numbers, 'UniformOutput', false);
```

```

% Convert the resulting cell array to a numeric array
numbers = cell2mat(numbers);

%% NY hitta regenerationer

Index2 = find(contains(LOGSEARCH,'Standard injection done.'));% stämmer med
portinject
%Index2 = find(contains(LOGSEARCH,'Unknown injection done.'));% stämmer med
portinject

text2= LOG(Index2,2);
text2=string(text2); %%%%%%%%%%%%%%% får ut rätt strings fortsatt här

% Use regexp to extract the numbers
numbers2 = regexp(text2, '\d+', 'match');

% Convert the cell array of strings to a numeric array
numbers2 = cellfun(@str2double,numbers2, 'UniformOutput', false);

% Convert the resulting cell array to a numeric array
numbers2 = cell2mat(numbers2);

x1= series0{:,1};
y1= series0{:,6};

x2=series1{:,1};
y2=series1{:,6};

figure (1)

plot(x1,y1,'r')
grid on

hold on

plot(x2,y2,'b')

hold on

v=numbers;
v2=numbers2;
% % Add vertical lines
line([v(1) v(1)], ylim, 'Color', 'k', 'LineStyle', '--')
line([v2(1) v2(1)], ylim, 'Color', 'g', 'LineStyle', '--')

for i = 2:length(v)
    line([v(i) v(i)], ylim, 'Color', 'k', 'LineStyle', '--')
end

hold on

% % Add vertical lines
for i = 2:length(v2)
    line([v2(i) v2(i)], ylim, 'Color', 'g', 'LineStyle', '--')
end

lgd = legend('Measured response electorde 1','Measured response electorde
2','Injections', 'Regenerations','location','southeast');
lgd.FontSize = 16;
xlabel 'Pulse'

```



```
ylabel 'Capacitance (pF)'  
set(gca,'FontSize',16)  
  
%Titel
```